

Electronic Supporting Information

Natural Born Laser Dyes: Excited-State Intramolecular Proton Transfer (ESIPT) Emitters and Their Use in Random Lasing Studies

Julien Massue,^{[a]*} Thibault Pariat,^[a] Pauline M. Vérité,^[b] Denis Jacquemin,^{[b]*} Martyna Durko,^[c] Tarek Chtouki,^[c] Lech Sznitko,^[c] Jaroslaw Mysliwiec^{[c]*} and Gilles Ulrich^[a]

S1. Synthetic schemes

S2. Experimental procedures

S3. ¹H and ¹³C NMR traces

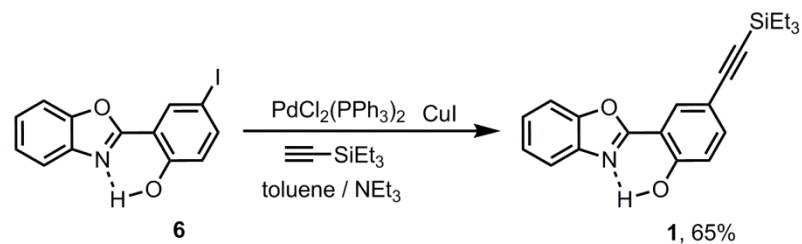
S4. HR-MS spectra

S5. Spectroscopic data

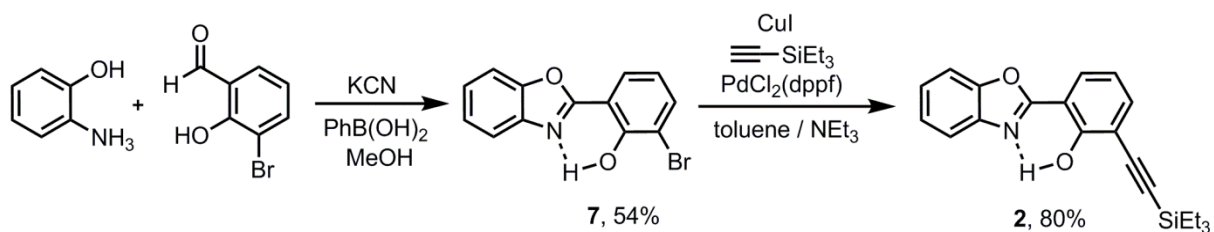
S6. Theoretical calculations

S7. Sample preparation for RL studies

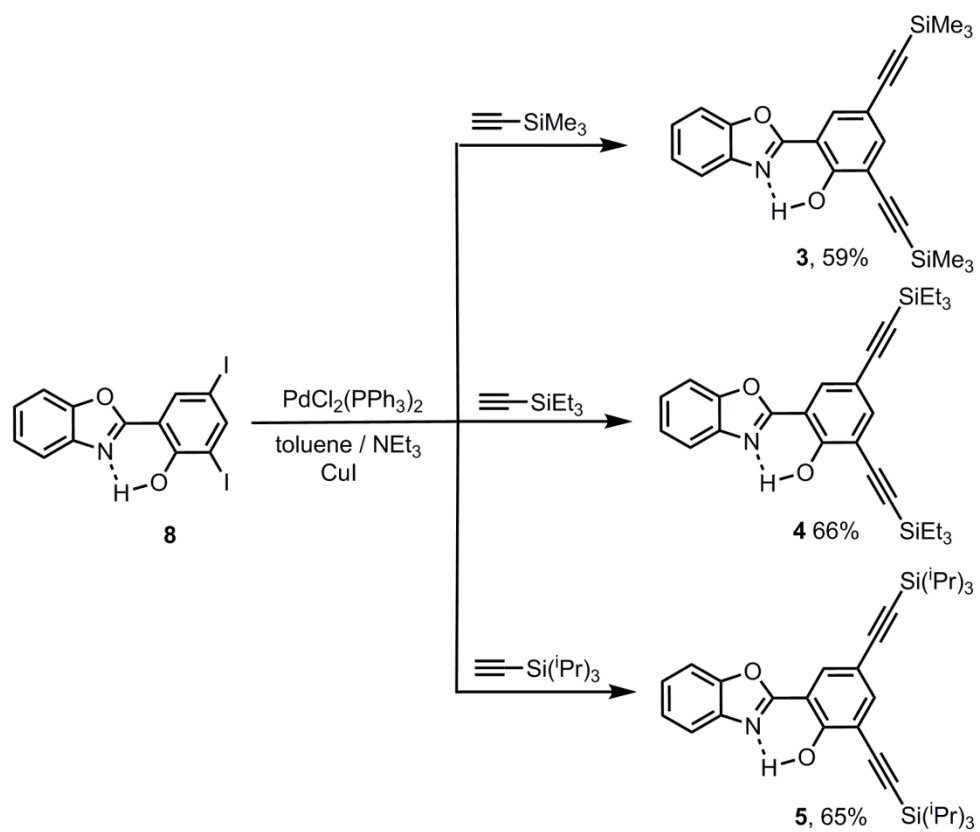
S1. Synthetic schemes



Scheme S1.1. Synthesis of HBO dye 1.



Scheme S1.2. Synthesis of HBO dye 2.



Scheme S1.3. Synthesis of HBO dyes **3**, **4** and **5**.

S2. Experimental procedures

Materials and methods

All reactions were performed under a dry atmosphere of argon. Chemicals were purchased from commercial sources and used without further purification. Reaction solvents were distilled according to common procedures. Thin layer chromatography (TLC) was performed on silica gel or aluminum oxide plates coated with fluorescent indicator. Chromatographic purifications were conducted using 40-63 μm silica gel. All mixtures of solvents are given in *v/v* ratio.

^1H NMR (400.1 MHz) and ^{13}C NMR (100.5 MHz) spectra were recorded on a Bruker Advance 400 MHz spectrometer, with perdeuterated solvents containing residual protonated solvent signals as internal references.

Absorption spectra were recorded using a dual-beam grating Shimadzu UV-3000 absorption spectrometer with a 1 cm quartz cell. The steady-state fluorescence emission and excitation spectra were obtained by using a Horiba S2 Jobin Yvon Fluoromax 4. All fluorescence spectra were corrected. Solvents for spectroscopy were spectroscopic grade and were used as received. All fluorescence spectra were corrected. The fluorescence quantum yield (Φ_{exp}) was calculated from Eq (1).

$$\Phi_{\text{exp}} = \Phi_{\text{ref}} \frac{I}{I_{\text{ref}}} \frac{\text{OD}_{\text{ref}}}{\text{OD}} \frac{\eta^2}{\eta_{\text{ref}}^2} \quad (\text{eq 1})$$

where I denotes the integral of the corrected emission spectrum, OD is the optical density at the excitation wavelength, and η is the refractive index of the medium. The quantum yield was determined in solution by using quinine sulfate as a reference ($\lambda_{\text{exc}} = 366 \text{ nm}$, $\Phi = 0.55$ in 1N H_2SO_4), for dyes emitting below 480 nm, Rhodamine 6G as a reference ($\lambda_{\text{exc}} = 488 \text{ nm}$, $\Phi =$

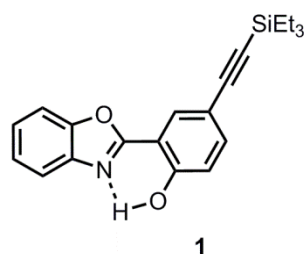
0.88 in ethanol), for dyes emitting between 480 and 570 nm or cresyl violet ($\lambda_{\text{exc}} = 546 \text{ nm}$, $\Phi = 0.55$ in ethanol) as a reference for dyes emitting above 570 nm.

Luminescence lifetimes were measured on an Edinburgh Instruments spectrofluorimeter equipped with a R928 photomultiplier and a PicoQuant PDL 800-D pulsed diode connected to a GwInstect GFG- 8015G delay generator. No filter was used for the excitation. Emission wavelengths were selected by a monochromator. Lifetimes were deconvoluted with FS-900 software using a light-scattering solution (LUDOX) for instrument response. The excitation source was a laser diode ($\lambda = 320 \text{ nm}$).

HBO dyes **3**, **6** and **8** were synthesized according to reported procedures.^{1,2}

Synthetic procedures

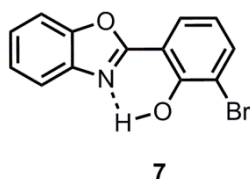
Synthesis of HBO 1



To a degassed solution of HBO 6 (1 eqt.) and Pd(PPh₃)₂Cl₂ (5 % mol.) in toluene and triethylamine (3/1, *v/v*), was added (triethylsilyl)acetylene (3 eqts.) and CuI (10 % mol.). The resulting mixture was stirred overnight at 90°C. After cooling down, it was extracted with CH₂Cl₂, washed with water three times. The organic

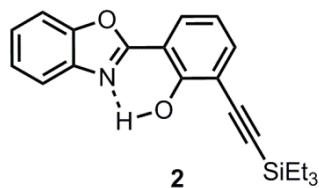
layers were dried over MgSO₄ and evaporated *in vacuo*. The product was purified by column chromatography on SiO₂ (CH₂Cl₂/ Pet. Ether. 1:9) to afford clean HBO 1 as a white powder. 65%. ¹H NMR (400MHz, CDCl₃) δ (ppm): 11.66 (s, 1H, OH), 8.16 (d, 1H, CH, ⁴J = 2Hz), 7.70-7.74 (m, 1H, CH), 7.59-7.63 (m, 1H, CH), 7.54 (dd, 1H, CH, ³J = 8.8Hz, ⁴J = 2Hz), 7.36-7.41 (m, 2H, CH), 7.05 (d, 1H, CH, ³J = 8.4Hz), 1.09 (t, 9H, CH₃, ³J = 7.6Hz), 0.71 (q, 6H, CH₂, ³J = 8.4Hz). ¹³C NMR (100.5Hz, CDCl₃) δ (ppm): 161.1, 157.7, 148.1, 138.8, 136.1, 129.9, 124.7, 124.2, 118.3, 116.6, 113.8, 109.7, 109.5, 104.3, 89.5, 6.5, 3.5. ESI-HRMS: calcd for C₂₁H₂₄NO₂Si: 350.1571 (M+H), found 350.1570 (M+H).

Synthesis of HBO 7



A mixture of 2-hydroxy-3-bromobenzaldehyde and 2-aminophenol (1 eqt) were refluxed in EtOH for 3 hours. An orange precipitate rapidly appeared that was filtered and further washed with EtOH before being redissolved in distilled CH₂Cl₂. 2,6-dichloro-3,5-dicyano-1,4-benzoquinone (DDQ) (1.2 eqt) was then added by portions and the resulting mixture stirred overnight at room temperature. The solvents were removed *in vacuo* and the crude mixture purified by column chromatography on SiO₂ (CH₂Cl₂/Pet. Ether. 1:9) to avoid HBO 7 as a white powder. 54%. ¹H NMR (400MHz, CDCl₃) δ (ppm): 12.27 (s, 1H, OH), 8.01 (dd, 1H, CH, ³J = 7.6Hz, ⁴J = 1.6Hz), 7.73-7.78 (m, 1H, CH), 7.70 (dd, 1H, CH, ³J = 7.6Hz, ⁴J = 1.6Hz), 7.60-7.65 (m, 1H, CH), 7.39-7.44 (m, 2H, CH), 6.93 (t, 1H, CH, ³J = 8Hz). ¹³C NMR (100.5Hz, CDCl₃) δ (ppm): 162.3, 155.6, 149.5, 139.8, 137.0, 126.5, 126.1, 125.5, 120.6, 119.7, 111.9, 111.5, 111.0. ESI-HRMS: calcd for C₁₃H₉BrNO₂: 291.9792 (M+H), found 291.9775 (M+H).

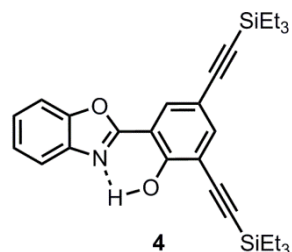
Synthesis of HBO 2



To a degassed solution of HBO 7 (1 eqt.) and Pd(PPh₃)₂Cl₂ (5 % mol.) in toluene and triethylamine (3/1, *v/v*), was added (triethylsilyl)acetylene (3 eqts.) and CuI (10 % mol.). The resulting mixture was stirred overnight at 90°C. After cooling down, it was

extracted with CH₂Cl₂, washed with water three times. The organic layers were dried over MgSO₄ and evaporated *in vacuo*. The product was purified by column chromatography on SiO₂ (CH₂Cl₂/ Pet. Ether. 1:9) to afford clean HBO 2 as a white powder. 80%. ¹H NMR (400MHz, CDCl₃) δ (ppm): 12.07 (s, 1H, OH), 8.00 (dd, 1H, CH, ³J = 8Hz, ⁴J = 1.6Hz), 7.70-7.75 (m, 1H, CH), 7.59-7.63 (m, 2H, CH), 7.37-7.42 (m, 2H, CH), 6.95 (t, 1H, CH, ³J = 7.6Hz), 1.10 (t, 9H, CH₃, ³J = 7.6 Hz), 0.73 (q, 6H, CH₂, ³J = 6.8 Hz). ¹³C NMR (100.5Hz, CDCl₃) δ (ppm): 162.5, 159.8, 149.2, 139.8, 137.5, 127.3, 125.6, 125.2, 119.4, 119.1, 112.8, 110.8, 110.7, 101.3, 97.3, 7.6, 4.5. ESI-HRMS: calcd for C₂₁H₂₄NO₂Si: 350.1571 (M+H), found 350.1576 (M+H).

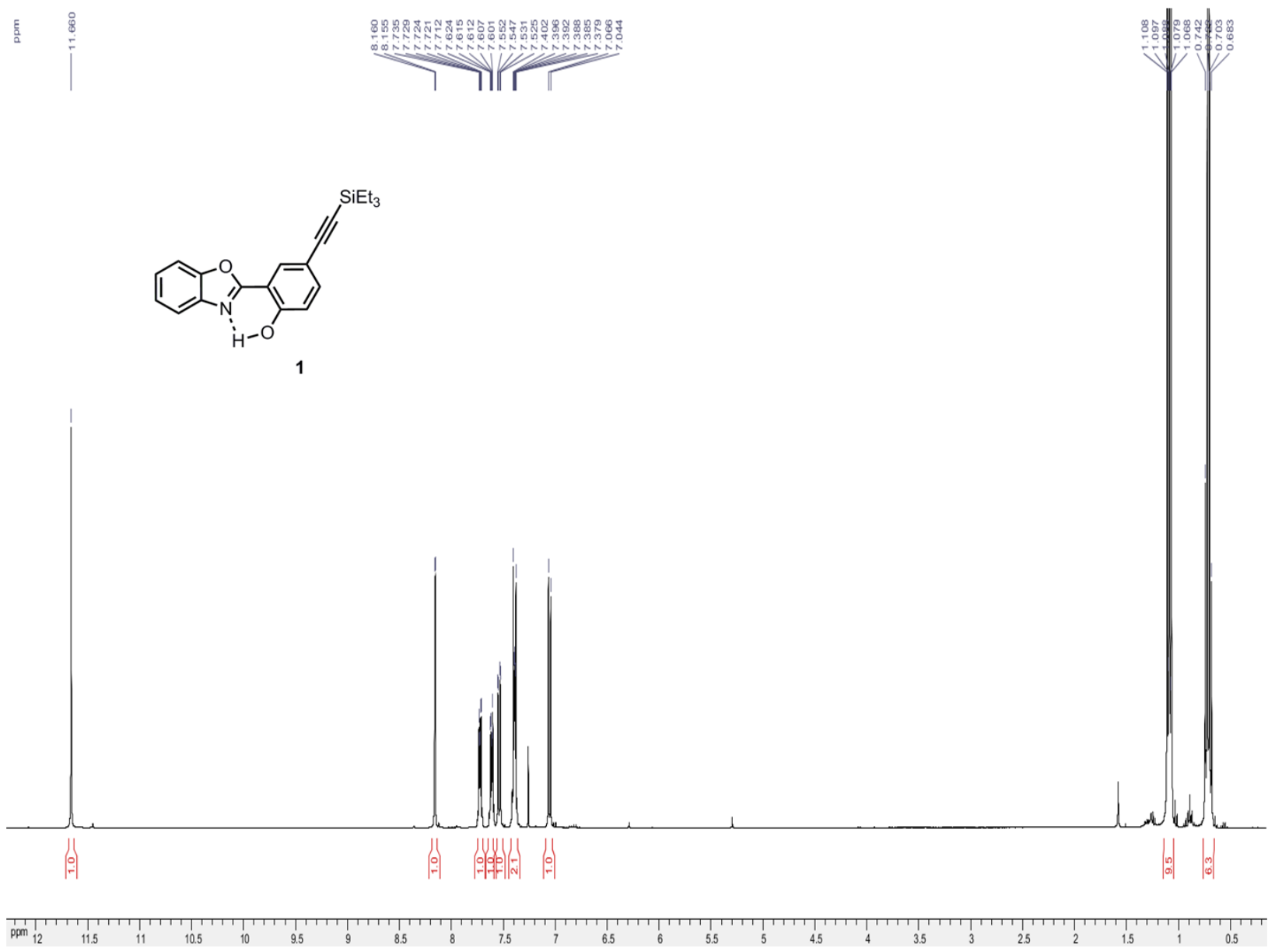
Synthesis of HBO 4



To a degassed solution of HBO 8 (1 eqt.) and Pd(PPh₃)₂Cl₂ (5 % mol.) in toluene and triethylamine (3/1, *v/v*), was added (triethylsilyl)acetylene (6 eqts.) and CuI (10 % mol.). The resulting mixture was stirred overnight at 90°C. After cooling down, it was extracted with CH₂Cl₂, washed with water three times. The organic

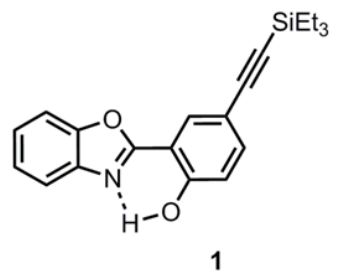
layers were dried over MgSO₄ and evaporated *in vacuo*. The product was purified by column chromatography on SiO₂ (CH₂Cl₂/ Pet. Ether. 1:9) to afford clean HBO 4 as a white powder. 66%. ¹H NMR (400MHz, CDCl₃) δ (ppm): 12.24 (s, 1H, OH), 8.10 (d, 1H, CH, ⁴J = 2Hz), 7.71-7.74 (m, 1H, CH), 7.70 (d, 1H, CH, ⁴J = 2Hz), 7.59-7.64 (m, 1H, CH), 7.37-7.43 (m, 2H, CH), 1.10 (t, 9H, CH₃, ³J = 7.6Hz), 1.08 (t, 9H, CH₃, ³J = 7.6Hz), 0.72 (q, 6H, CH₂, ³J = 8.4Hz), 0.70 (q, 6H, CH₂, ³J = 12Hz). ¹³C NMR (100.5Hz, CDCl₃) δ (ppm): 161.7, 159.7, 149.2, 140.5, 139.6, 130.7, 125.9, 125.3, 119.5, 114.6, 113.2, 110.8, 104.5, 100.3, 97.9, 91.1, 7.6, 4.5. ESI-HRMS: calcd for C₂₉H₃₈NO₂Si₂: 488.2436 (M+H), found 488.2438 (M+H).

S3 ¹H and ¹³C NMR traces

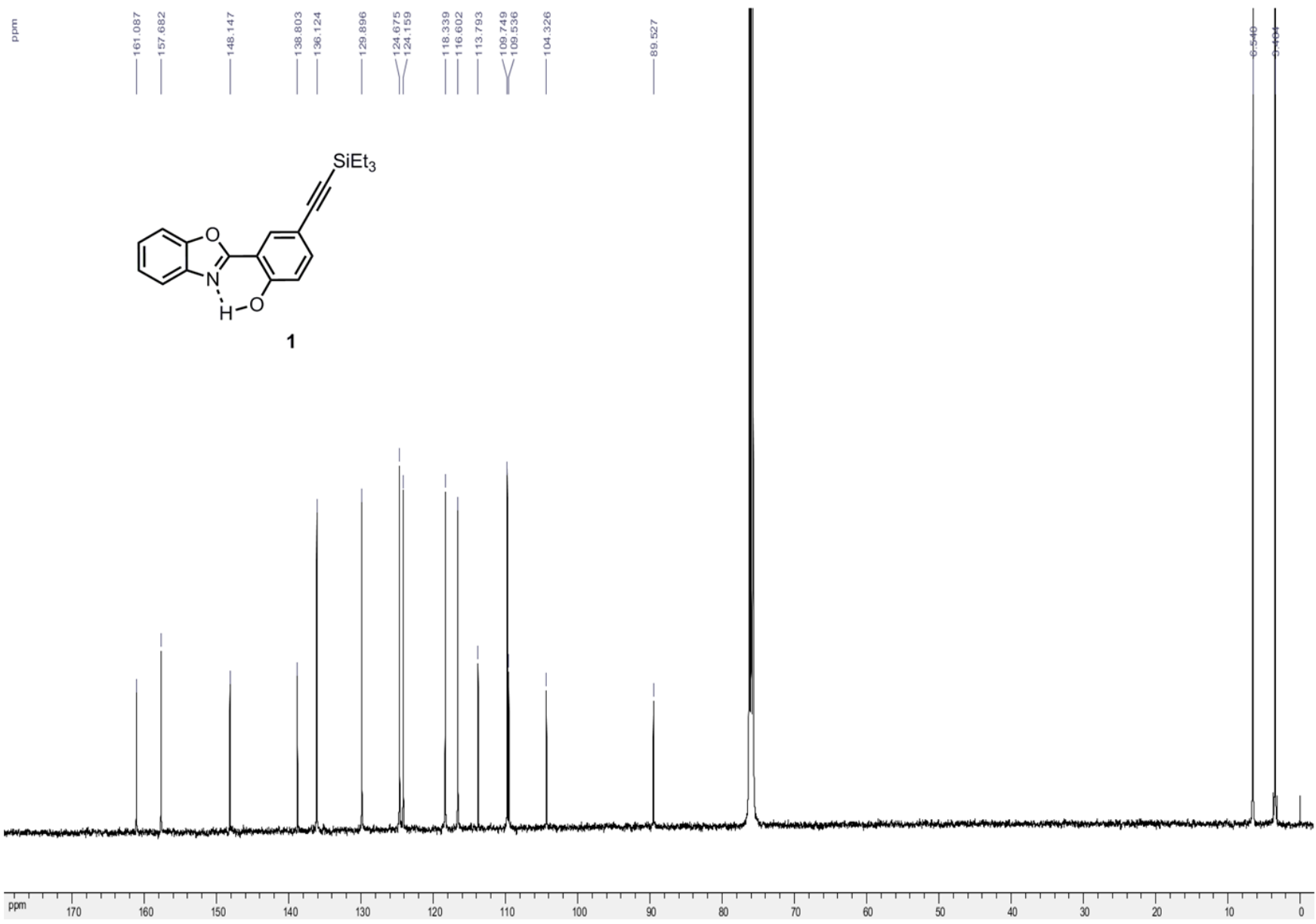


ppm

- 161.087
- 157.682
- 148.147
- 138.803
- 136.124
- 129.896
- 124.675
- 124.159
- 118.339
- 116.602
- 113.793
- 109.749
- 109.536
- 104.326



89.527

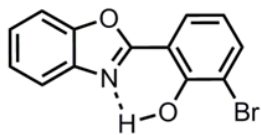


6.549

5.464

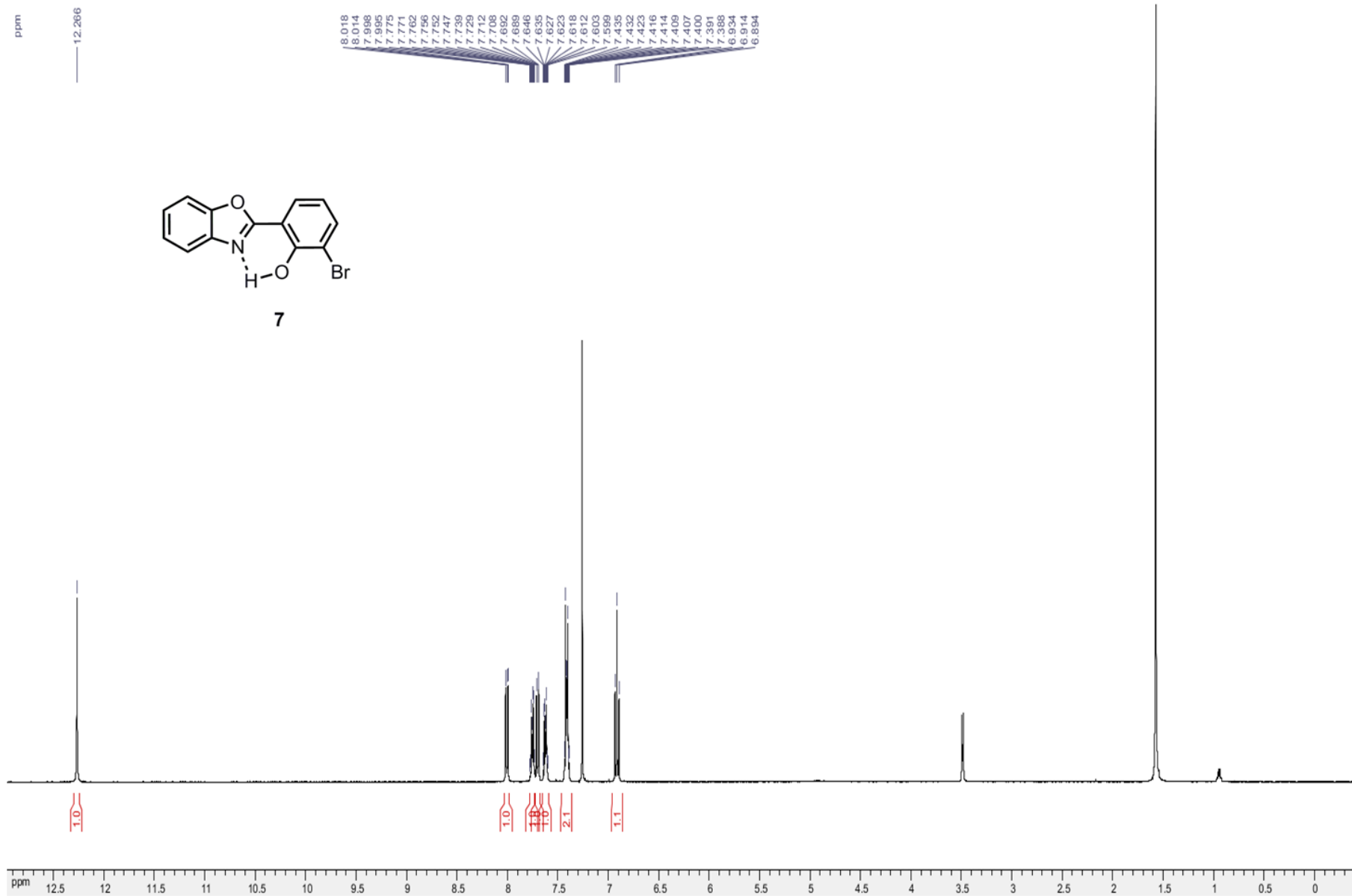
ppm

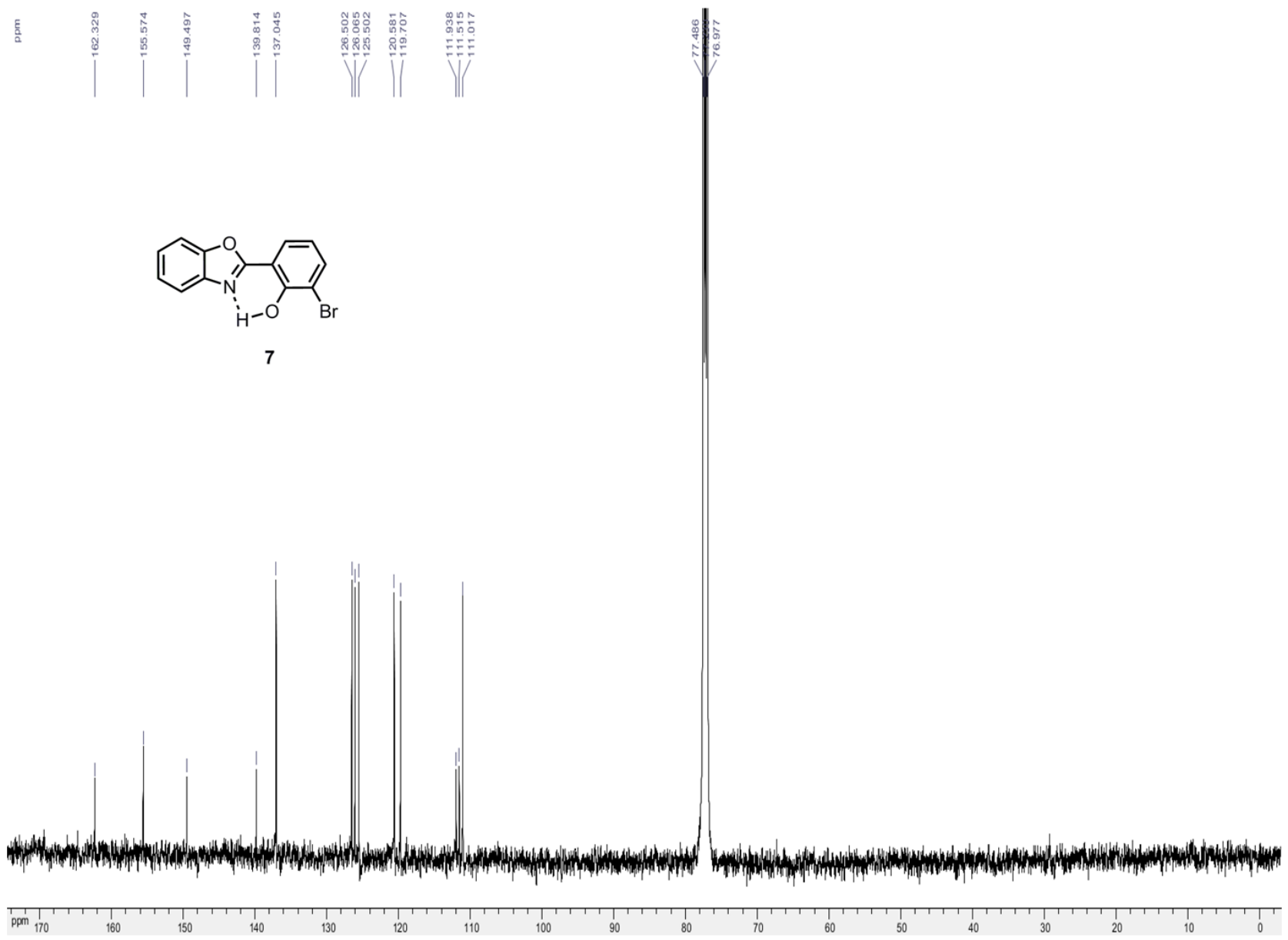
12.266

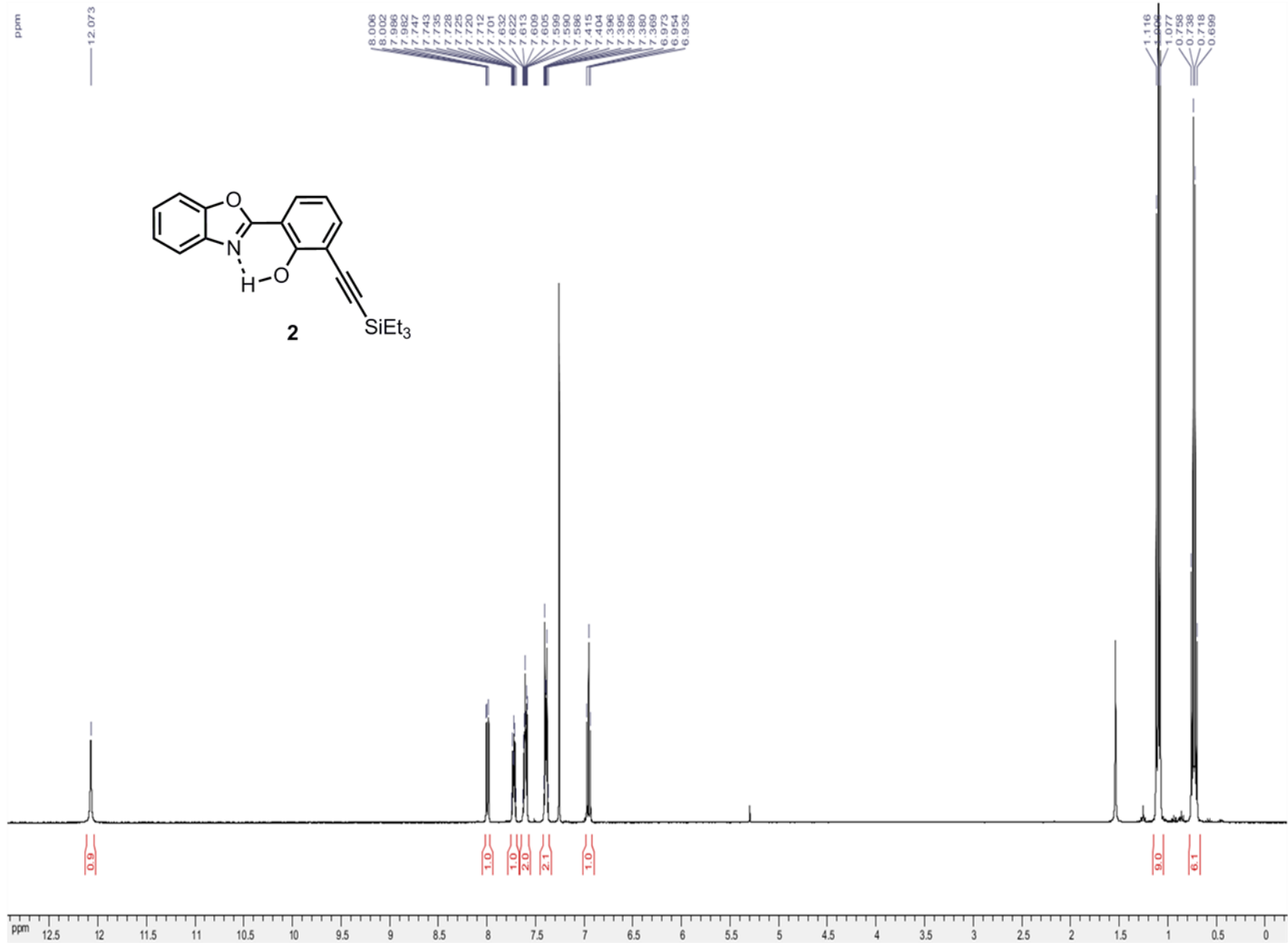


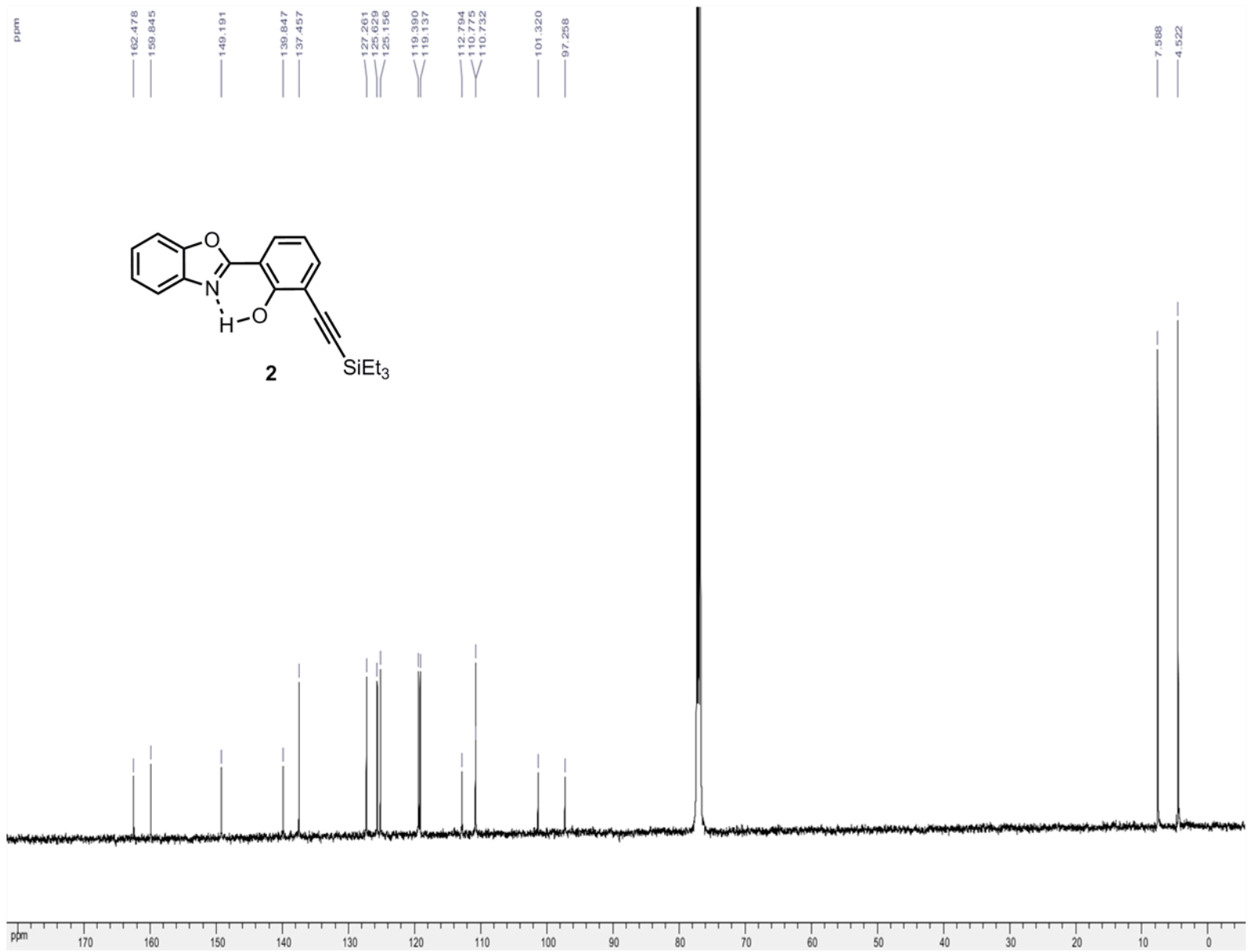
7

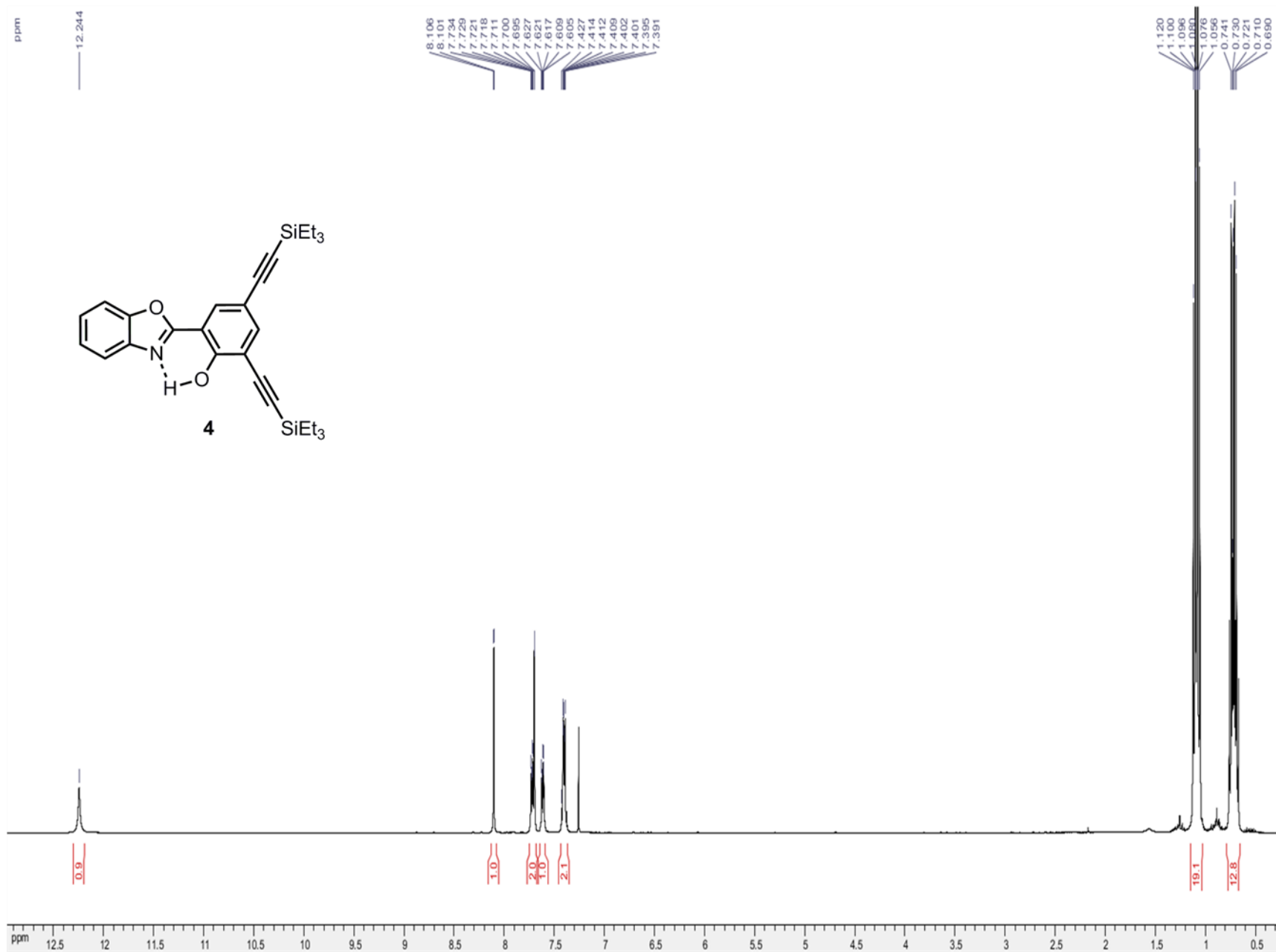
8.018
8.014
7.988
7.985
7.775
7.762
7.756
7.752
7.747
7.739
7.729
7.712
7.708
7.692
7.689
7.646
7.635
7.627
7.623
7.618
7.612
7.603
7.599
7.435
7.432
7.416
7.414
7.409
7.407
7.400
7.391
7.388
6.934
6.914
6.894

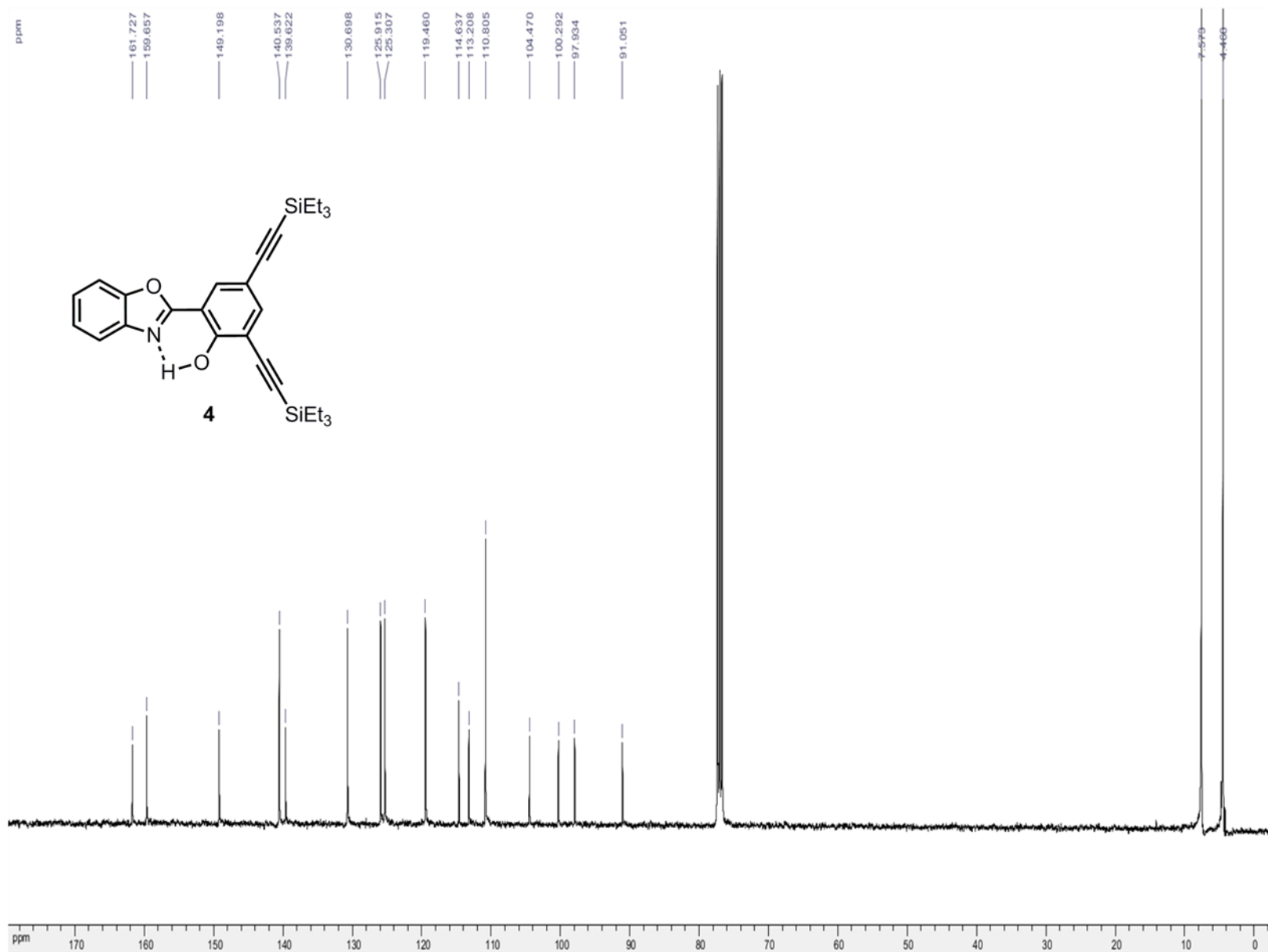


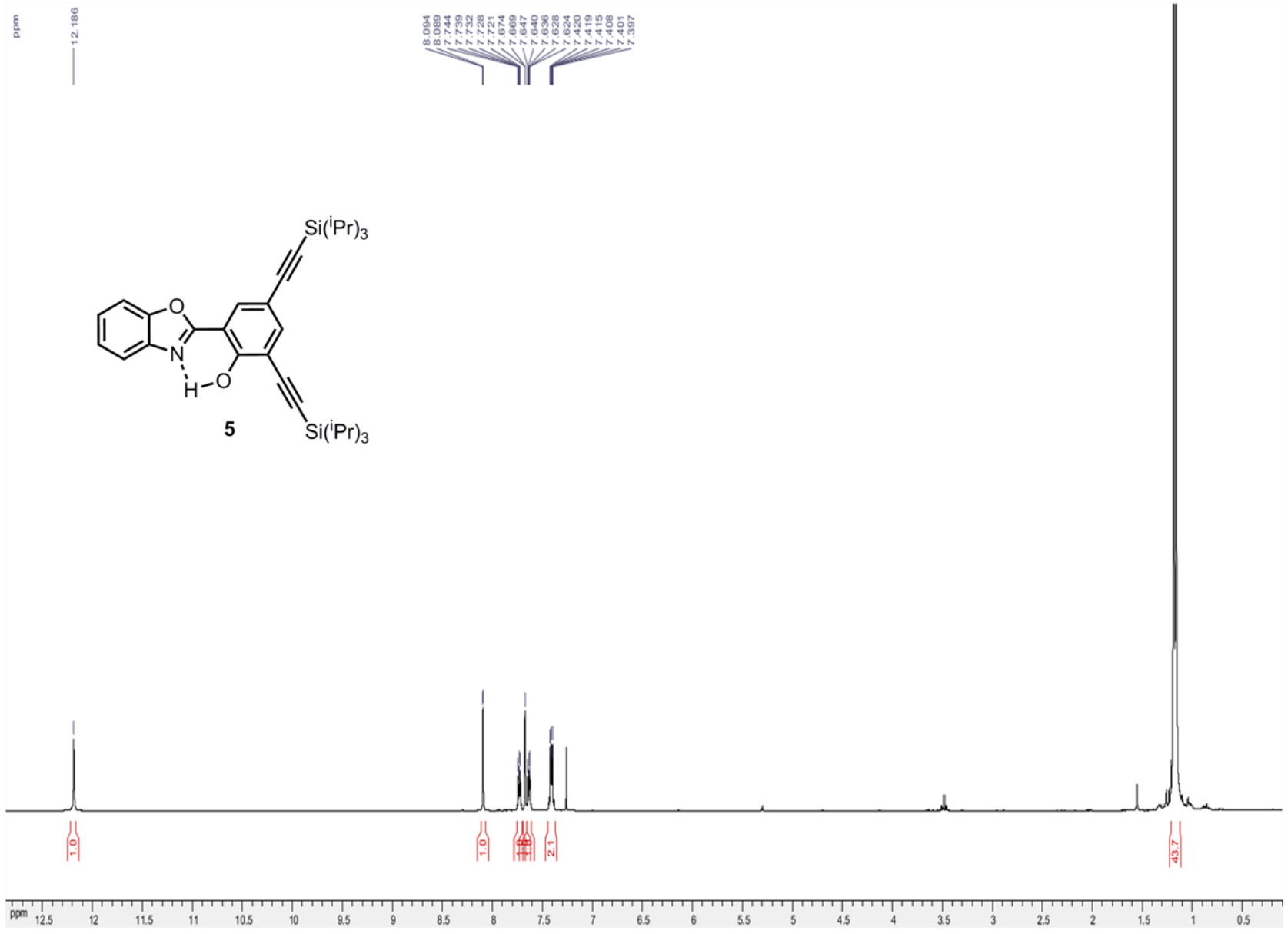


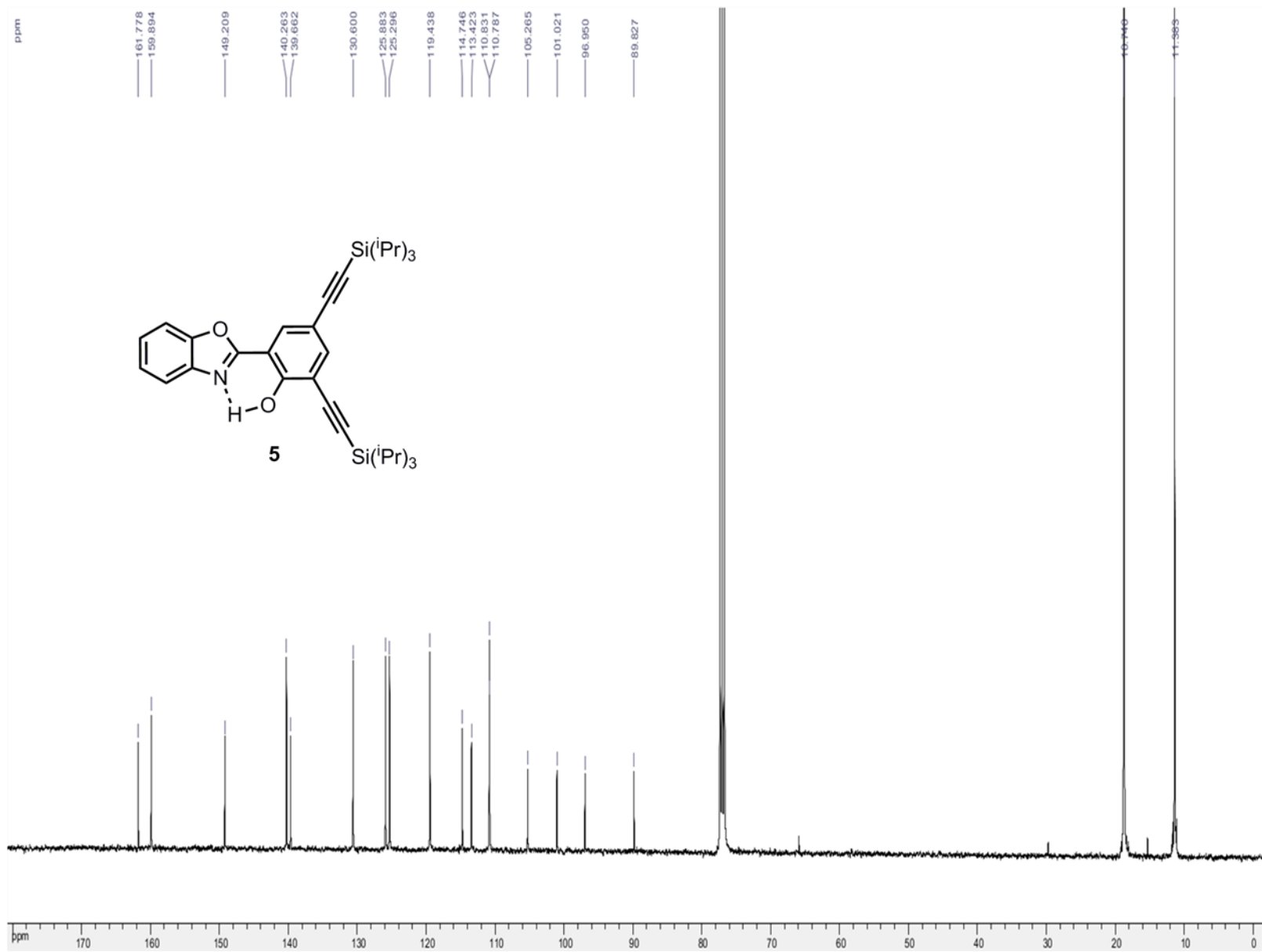




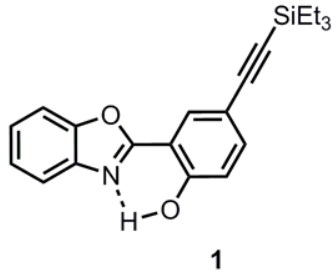








S4 HRMS spectra



Mass Spectrum HR Report

a\SM 2017\F00513SK.d
pos_Standard.m

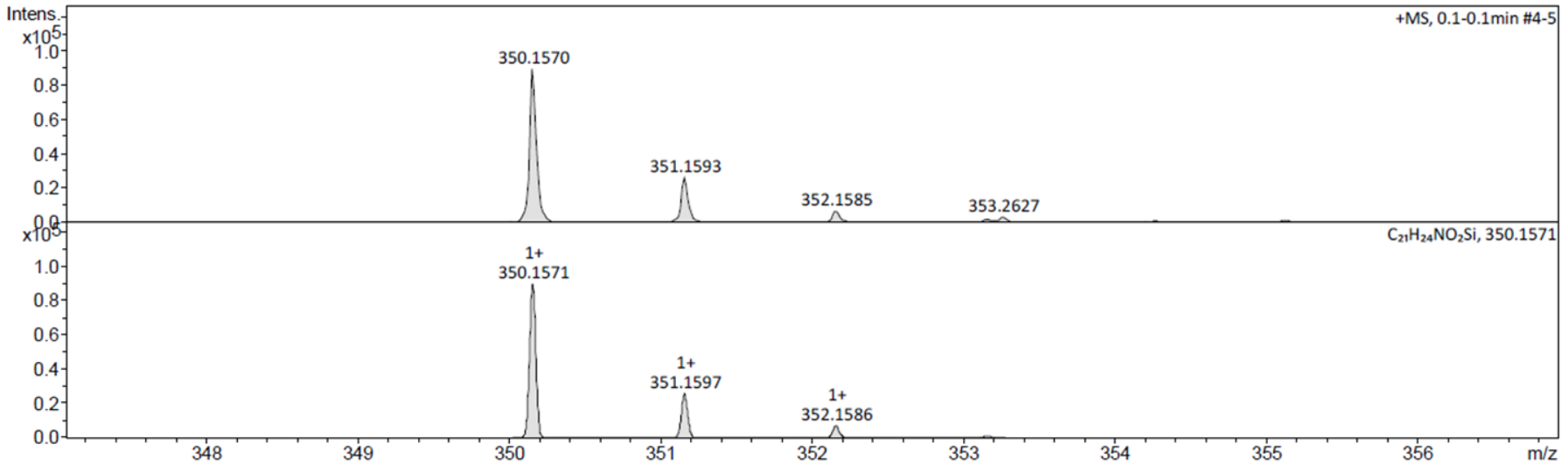
Acquisition Date	5/30/2017 1:50:26 PM
Operator	BDAL@DE
Instrument	micrOTOF II
	8213750.1045 1

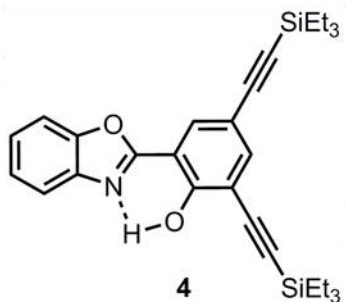
Acquisition Parameter

Source Type	ESI
n/a	n/a
Scan Begin	50 m/z
Scan End	3000 m/z

Ion Polarity	Positive
n/a	n/a

Set Corrector Fill	59.0 V
n/a	n/a
n/a	n/a
Set Reflector	1800.0 V
Set Flight Tube	8600.0 V
Set Detector TOF	1953.3 V





Mass Spectrum Molecular Formula Report

Service masse 2017\O41805SK.d
pos.m

Acquisition Date 3/10/2017 9:47:50 AM

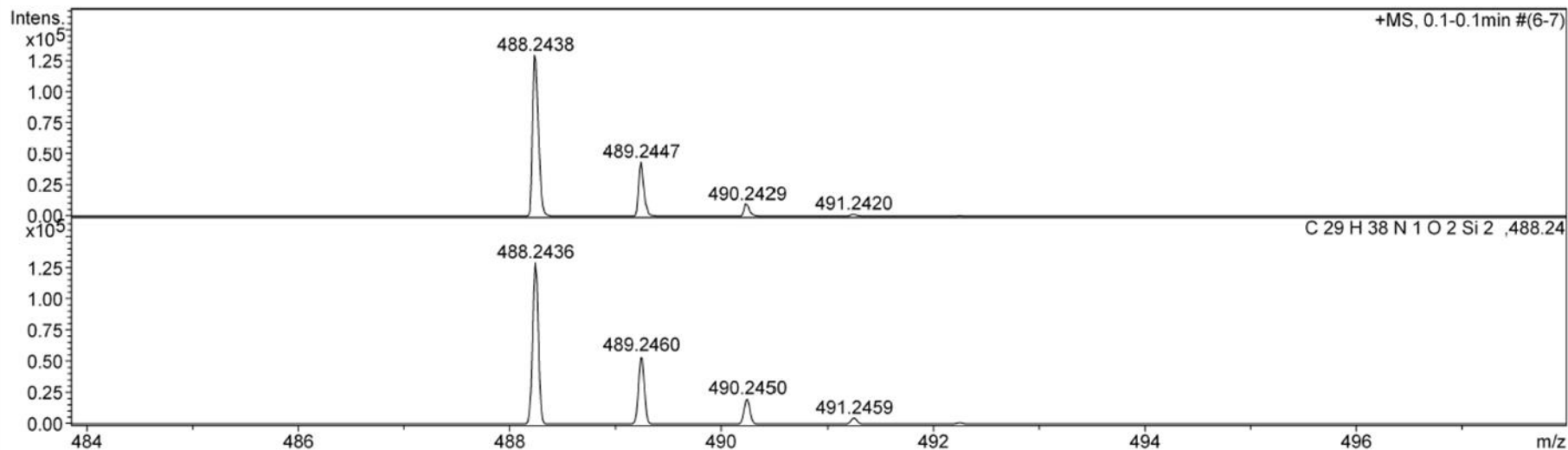
Operator Administrator
Instrument micrOTOF 66

Acquisition Parameter

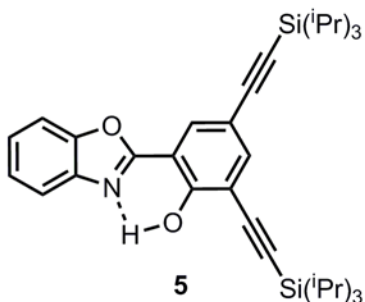
Source Type ESI
Scan Range n/a
Scan Begin 50 m/z
Scan End 3000 m/z

Ion Polarity Positive
Capillary Exit 150.0 V
Hexapole RF 220.0 V
Skimmer 1 50.0 V
Hexapole 1 24.3 V

Set Corrector Fill 57 V
Set Pulsar Pull 811 V
Set Pulsar Push 811 V
Set Reflector 1700 V
Set Flight Tube 8600 V
Set Detector TOF 1950 V



Sum Formula	Sigma	m/z	Err [ppm]	Mean Err [ppm]	rdb	N Rule	e ⁻
C 29 H 38 N 1 O 2 Si 2	0.06	488.2436	-0.40	1.11	13.50	ok	even
C 29 H 37 N 1 O 2 Si 2	0.58	487.2357	-11.46	-12.08	14.00	-	odd



Mass Spectrum Molecular Formula Report

.Service masse 2017\O41927SK.d
pos.m

Acquisition Date 3/21/2017 3:03:40 PM

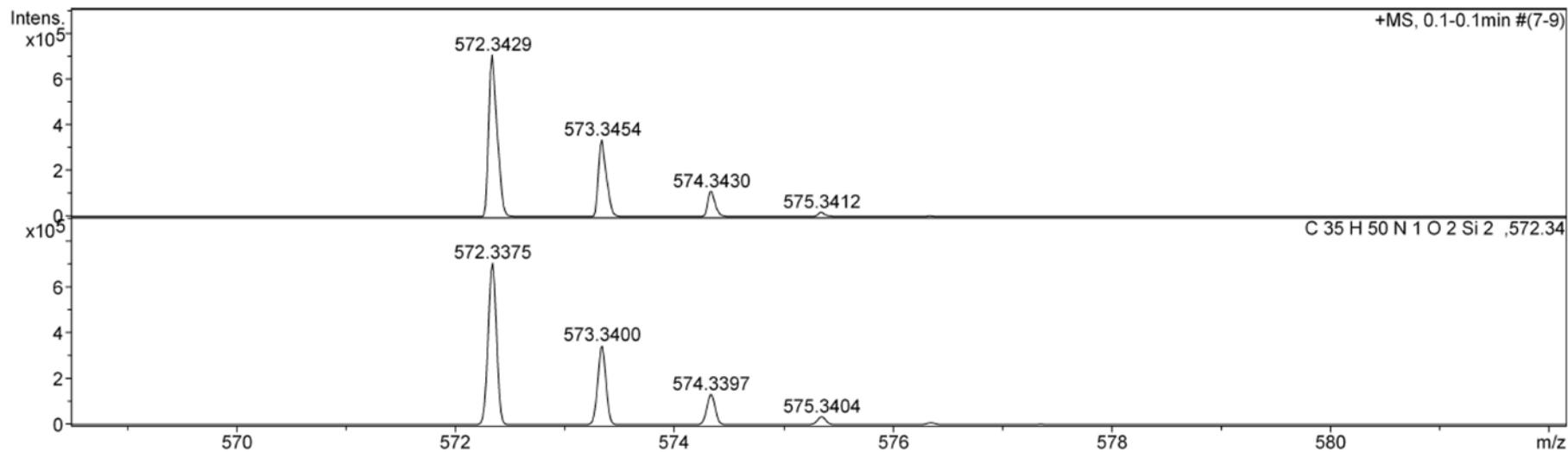
Operator Administrator
Instrument microTOF 66

Acquisition Parameter

Source Type ESI
Scan Range n/a
Scan Begin 50 m/z
Scan End 3000 m/z

Ion Polarity Positive
Capillary Exit 150.0 V
Hexapole RF 220.0 V
Skimmer 1 50.0 V
Hexapole 1 24.3 V

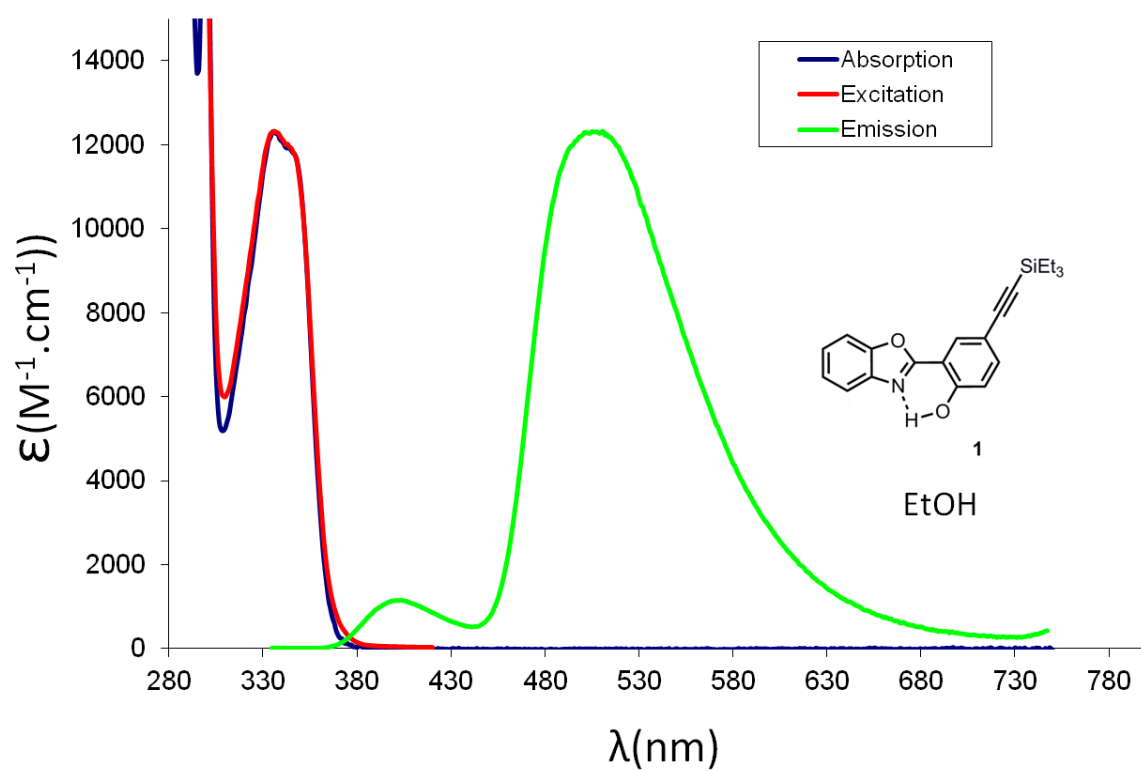
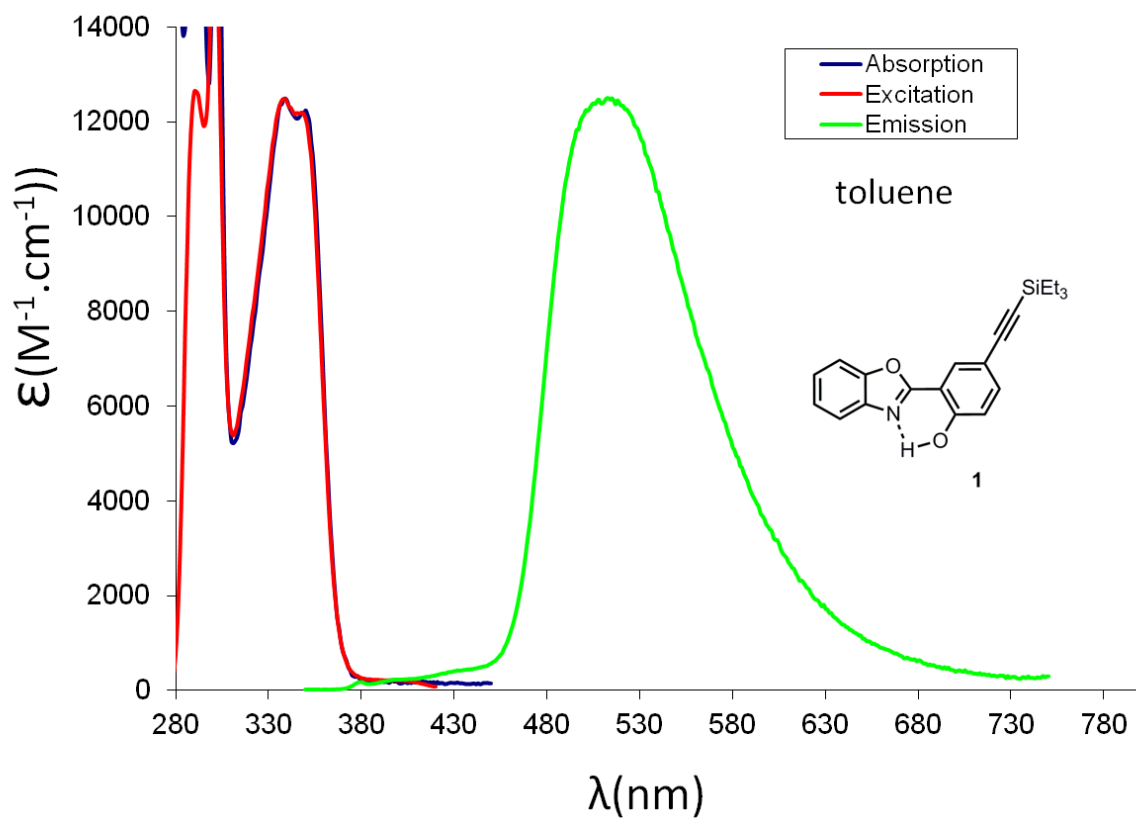
Set Corrector Fill 57 V
Set Pulsar Pull 811 V
Set Pulsar Push 811 V
Set Reflector 1700 V
Set Flight Tube 8600 V
Set Detector TOF 1950 V

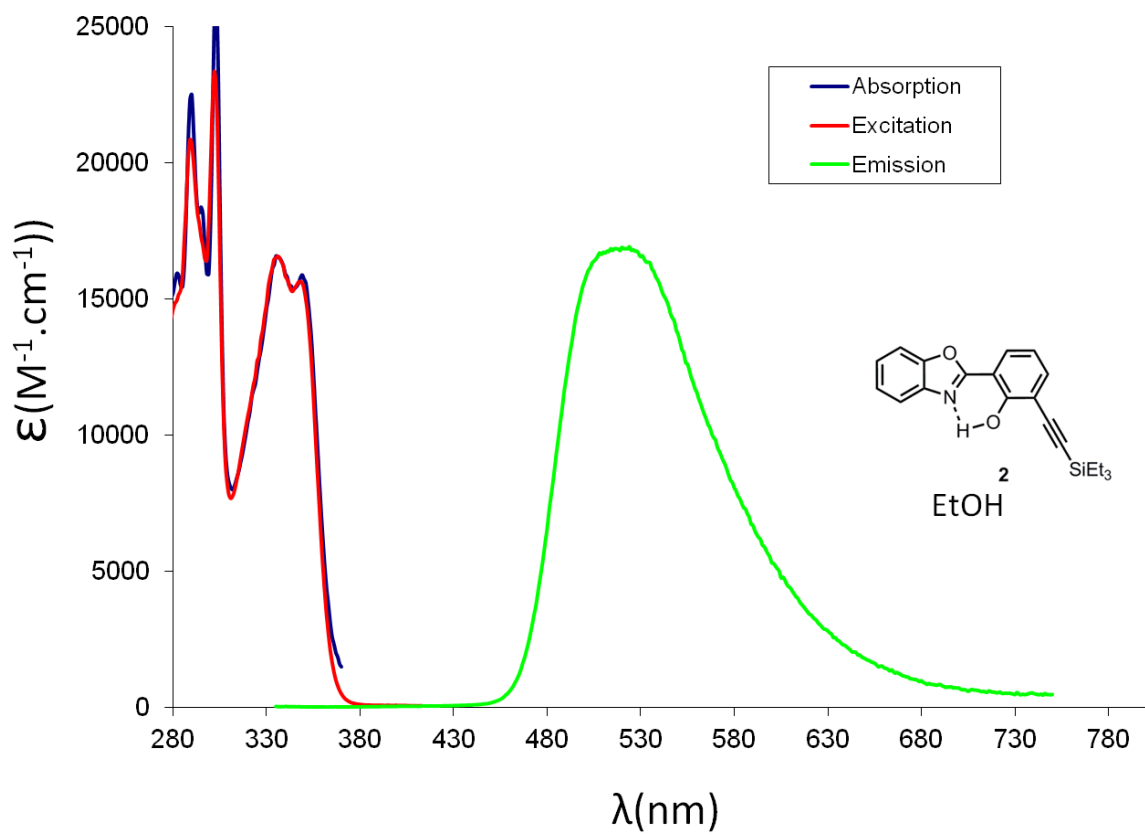
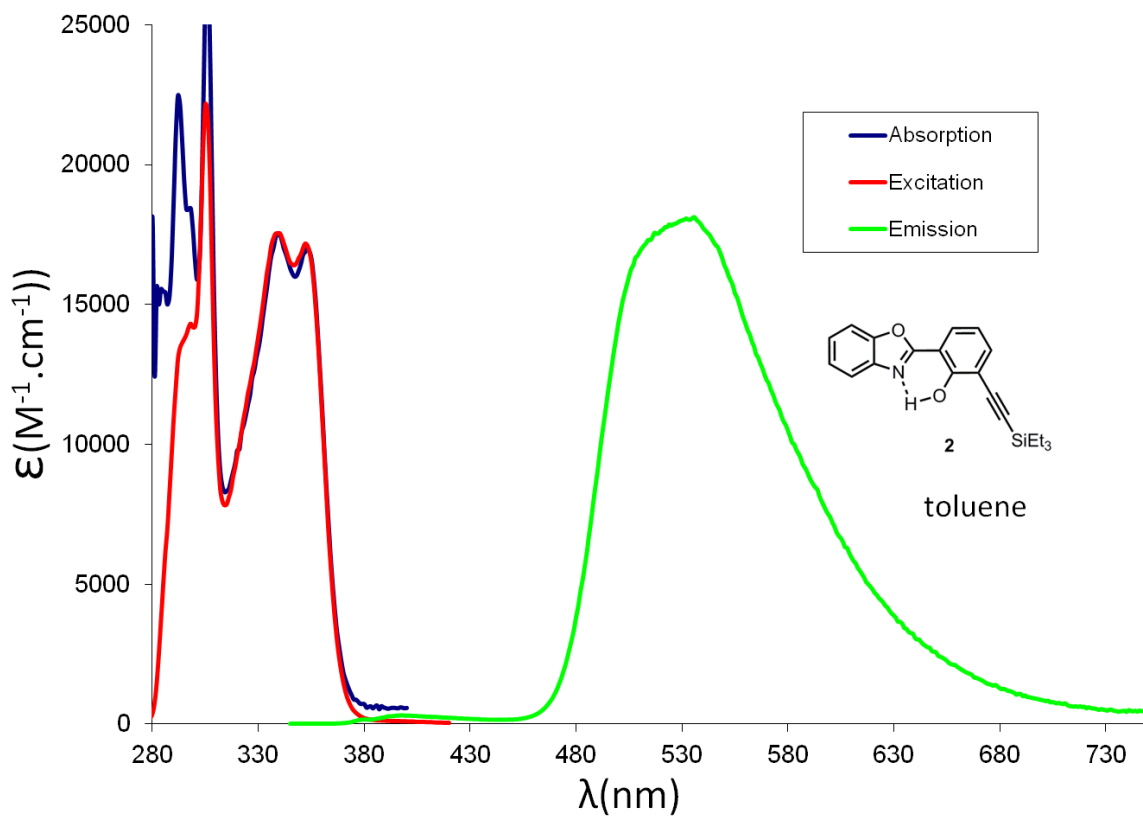


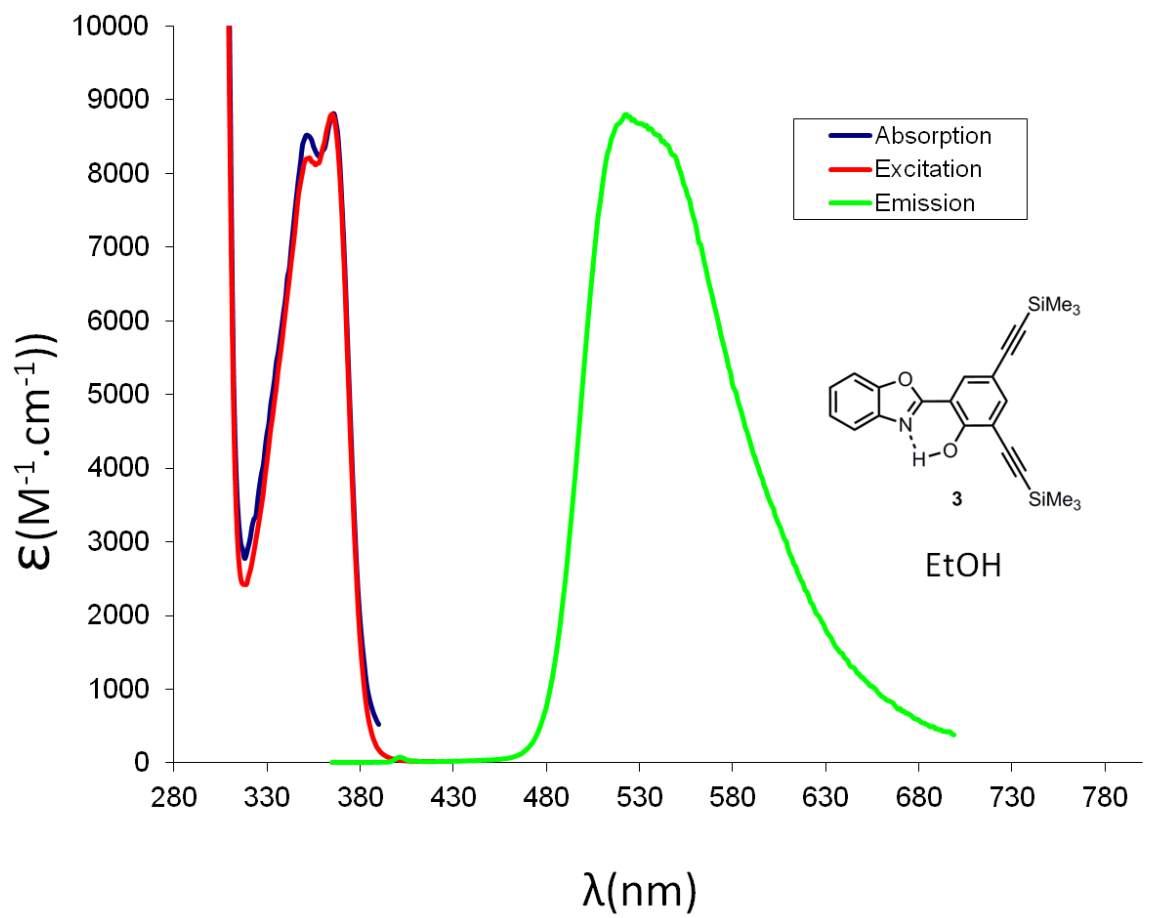
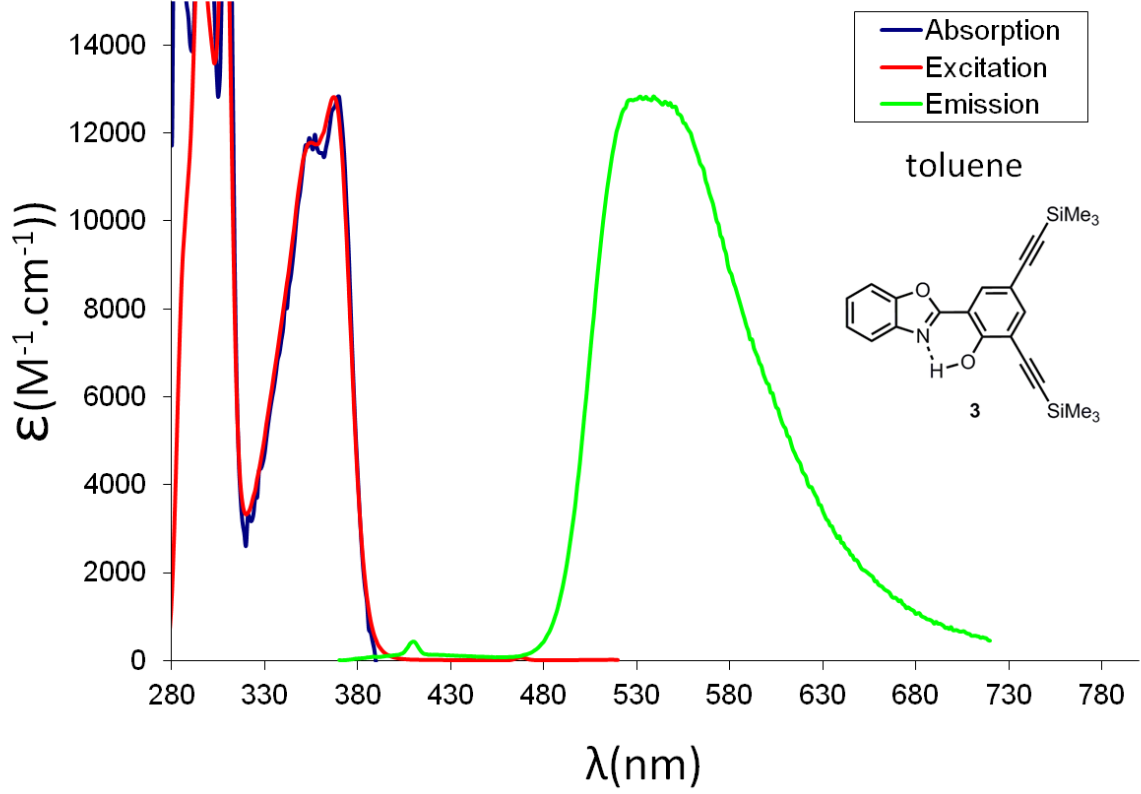
Sum Formula	Sigma	m/z	Err [ppm]	Mean Err [ppm]	rdb	N Rule	e ⁻
C 35 H 50 N 1 O 2 Si 2	0.02	572.3375	-9.58	-8.75	13.50	ok	even

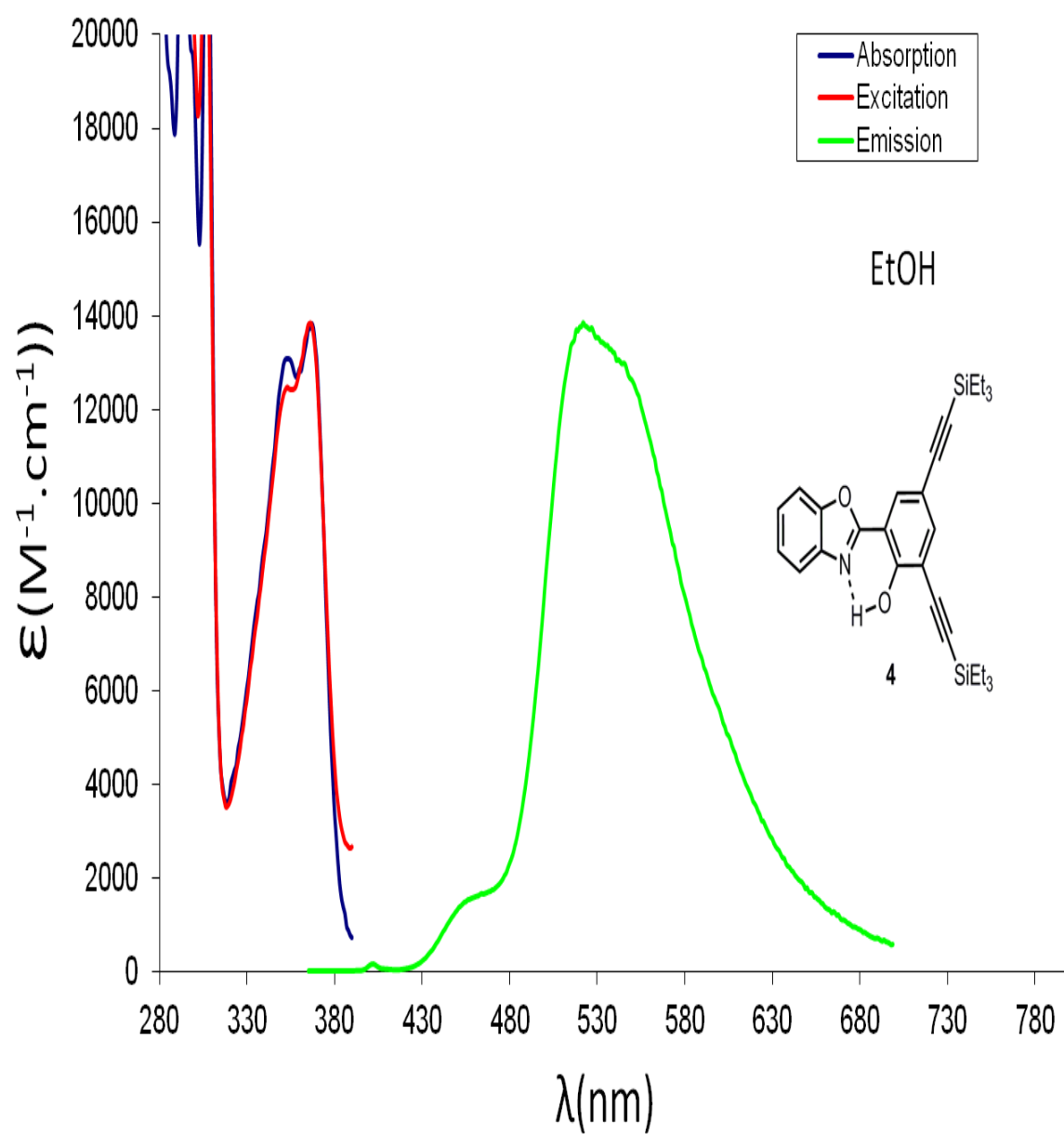
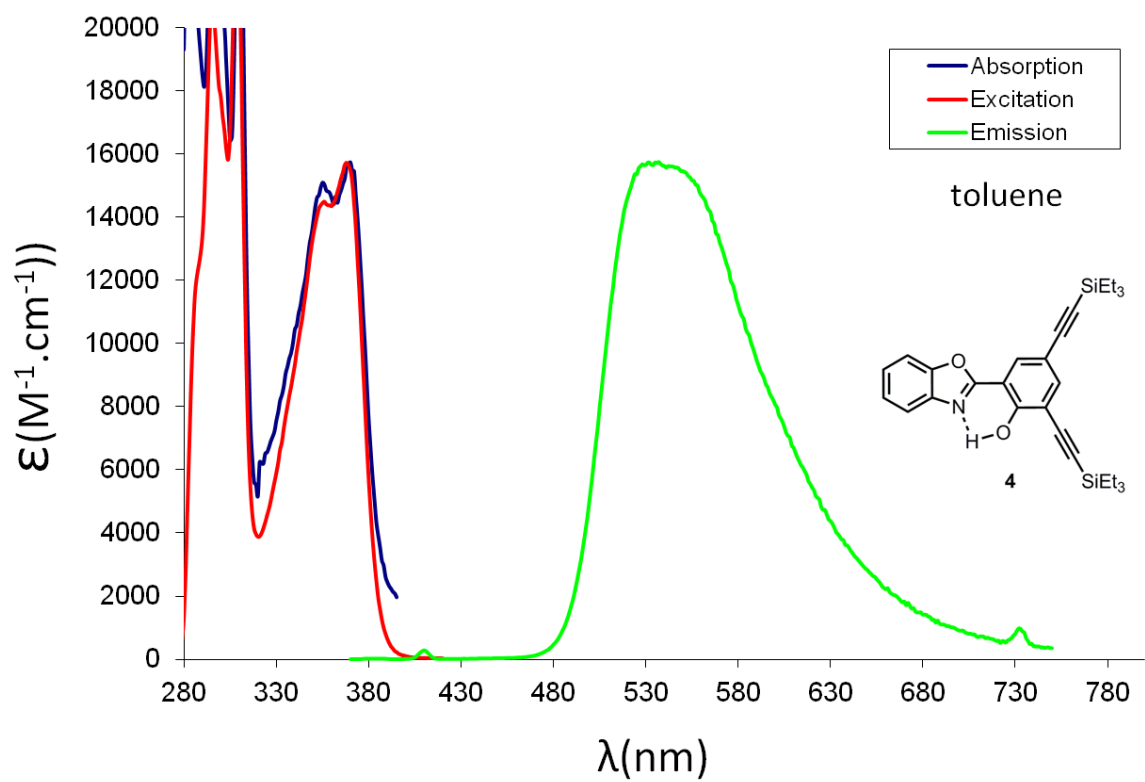
S5 Spectroscopic data

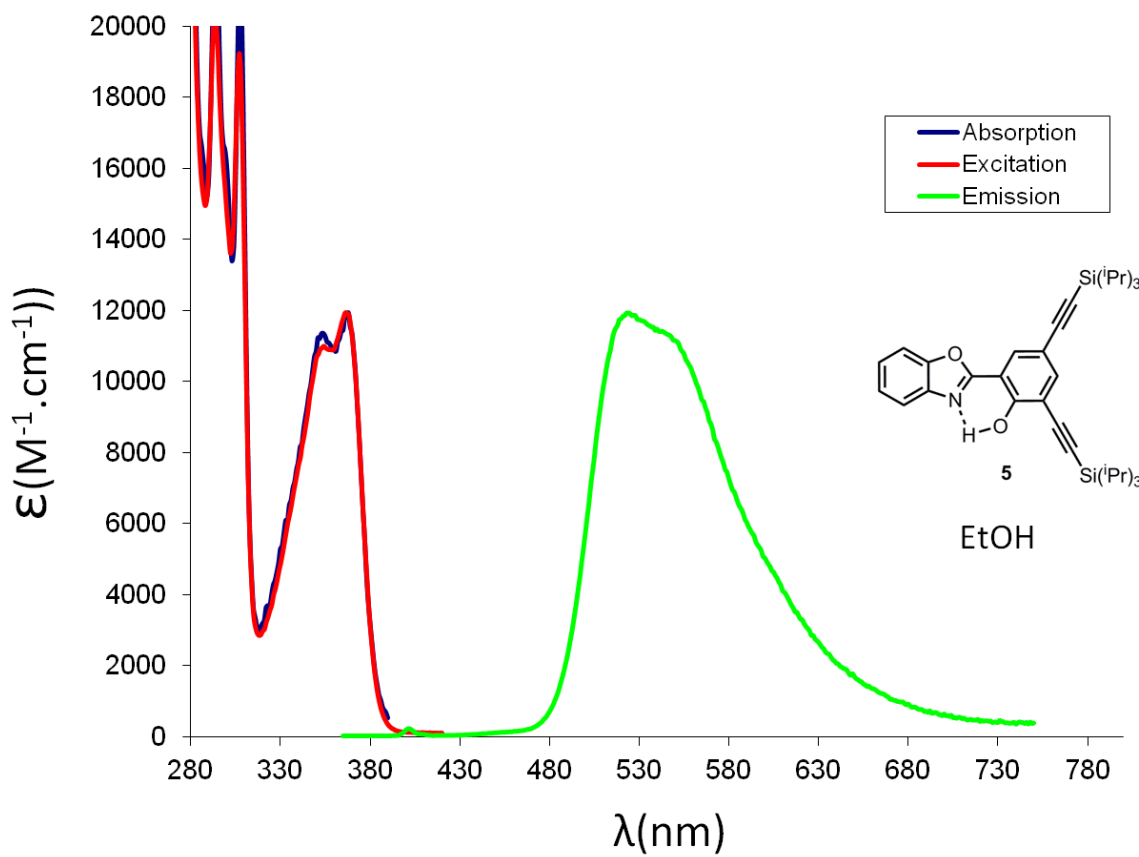
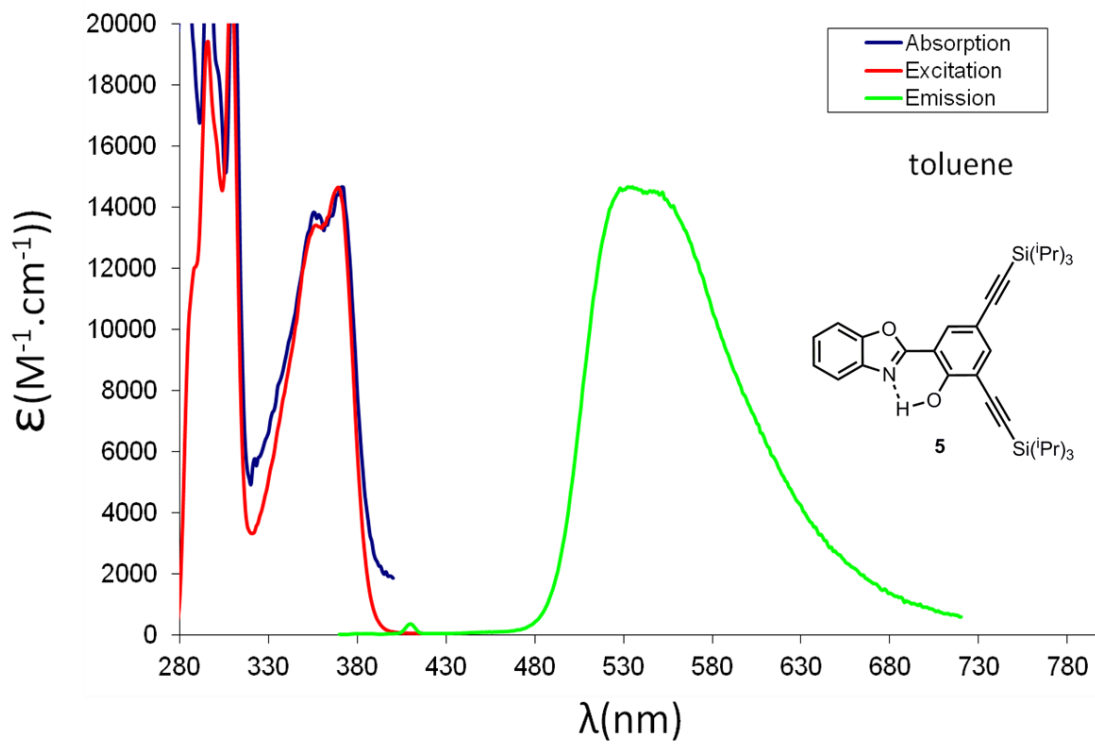
S5.1 Absorption, emission and excitation spectra of HBO dyes 1-5 in solution at 25°C



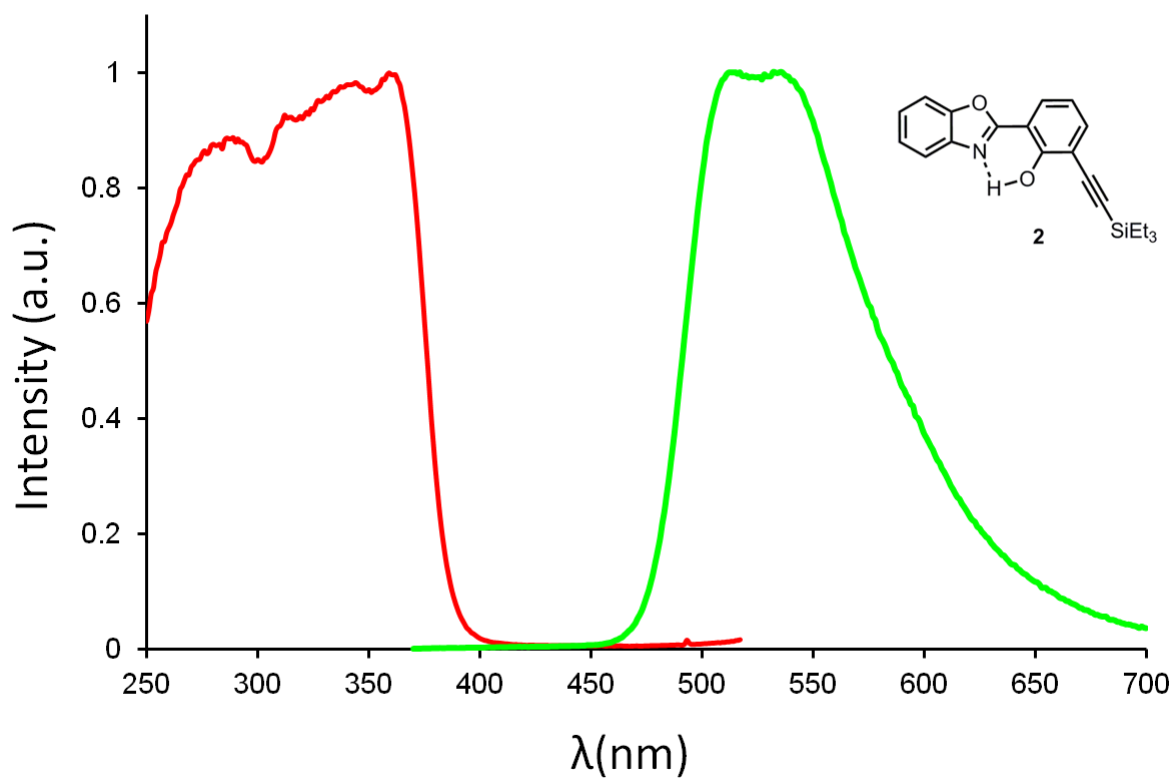
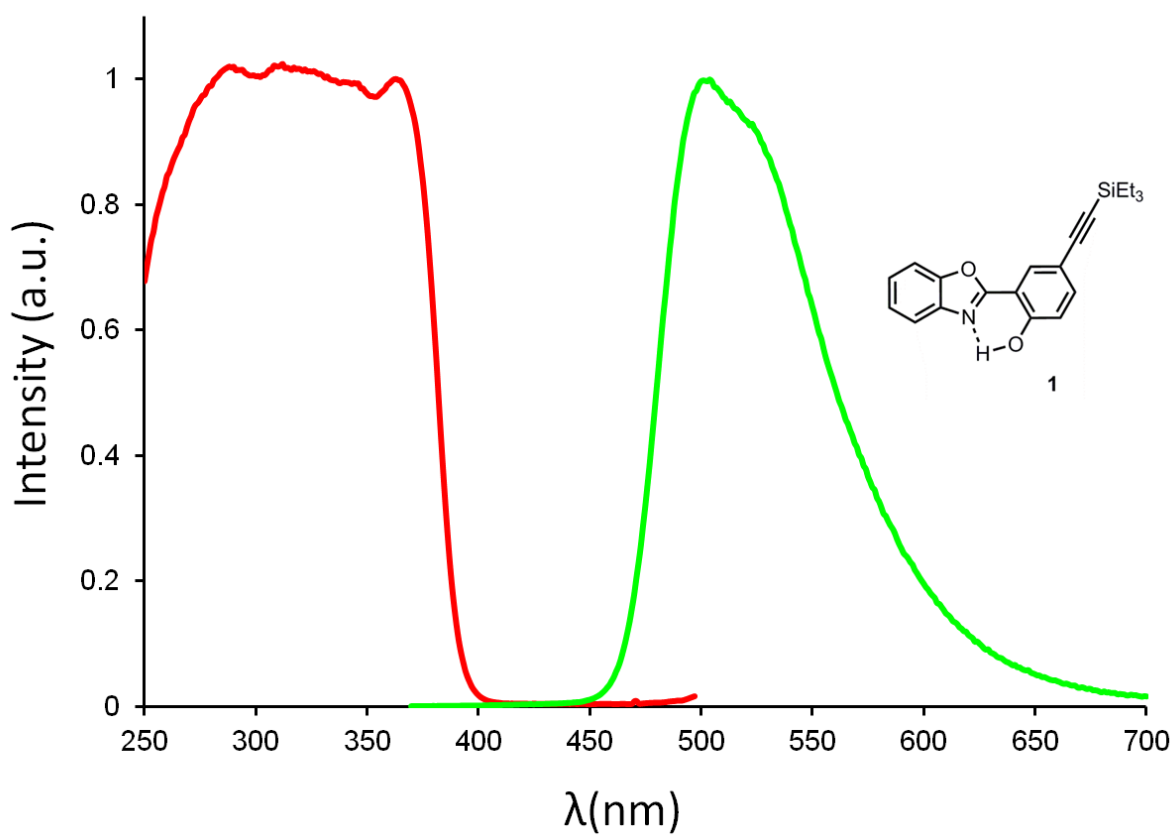


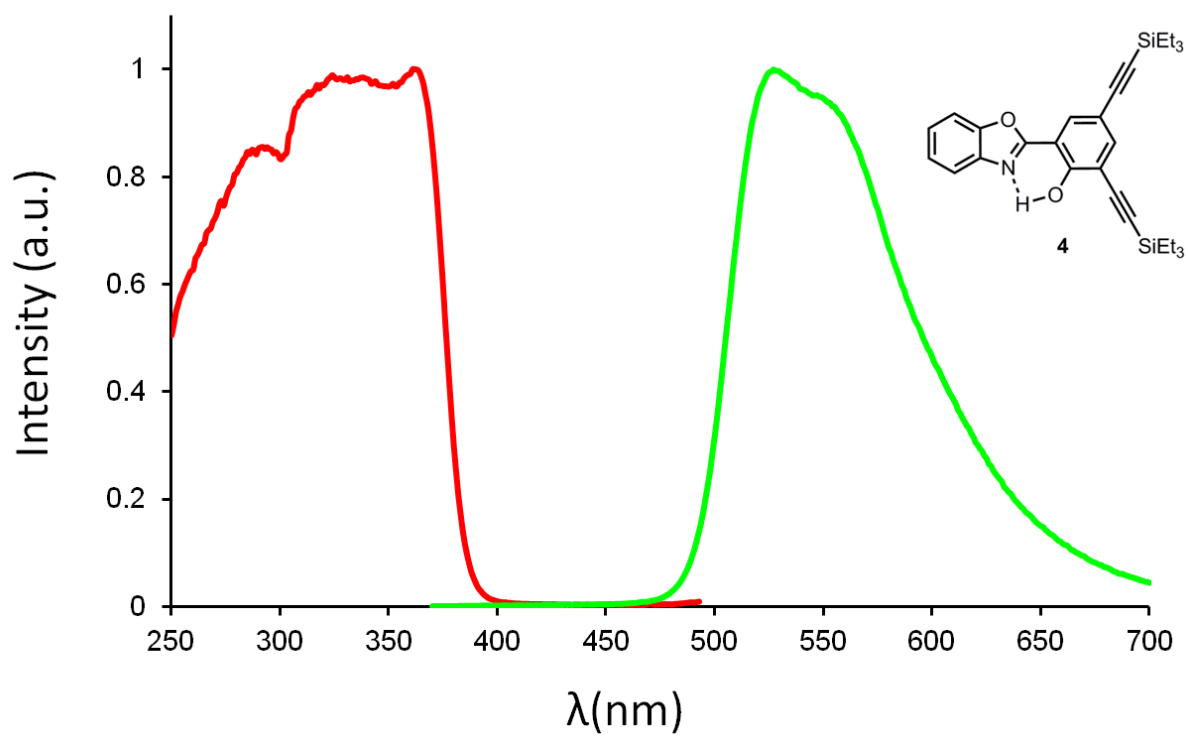
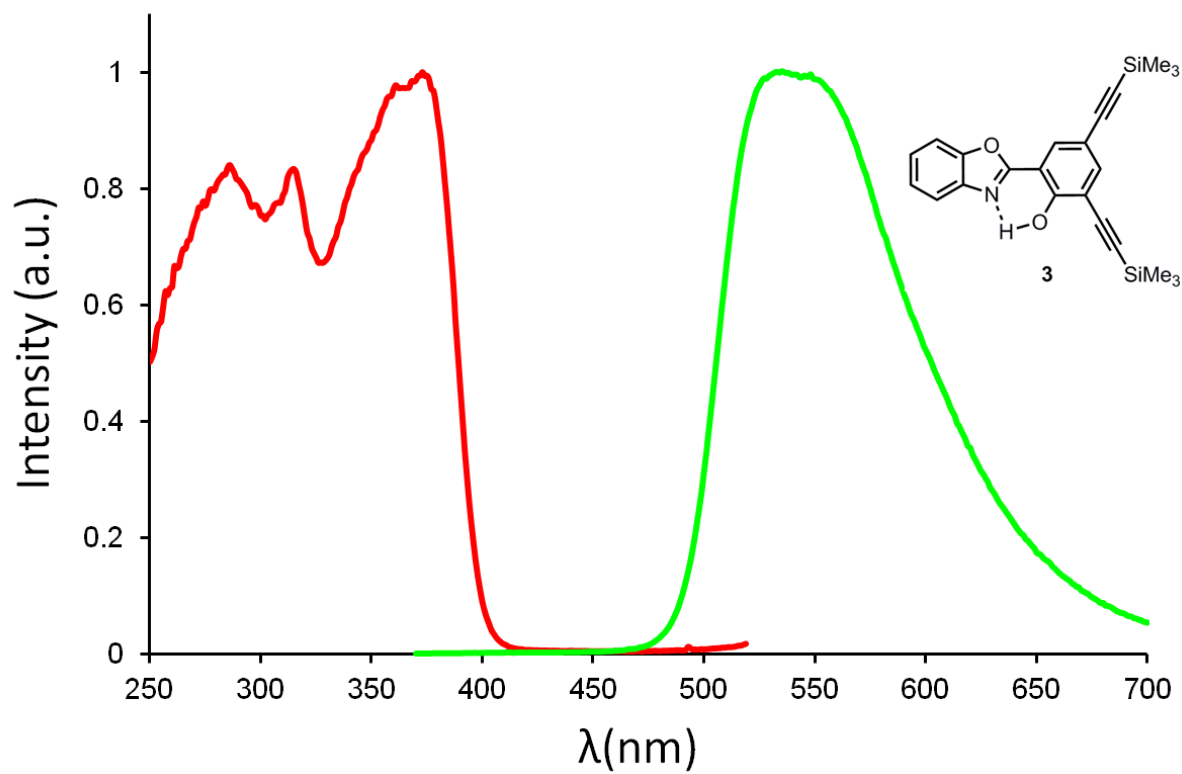


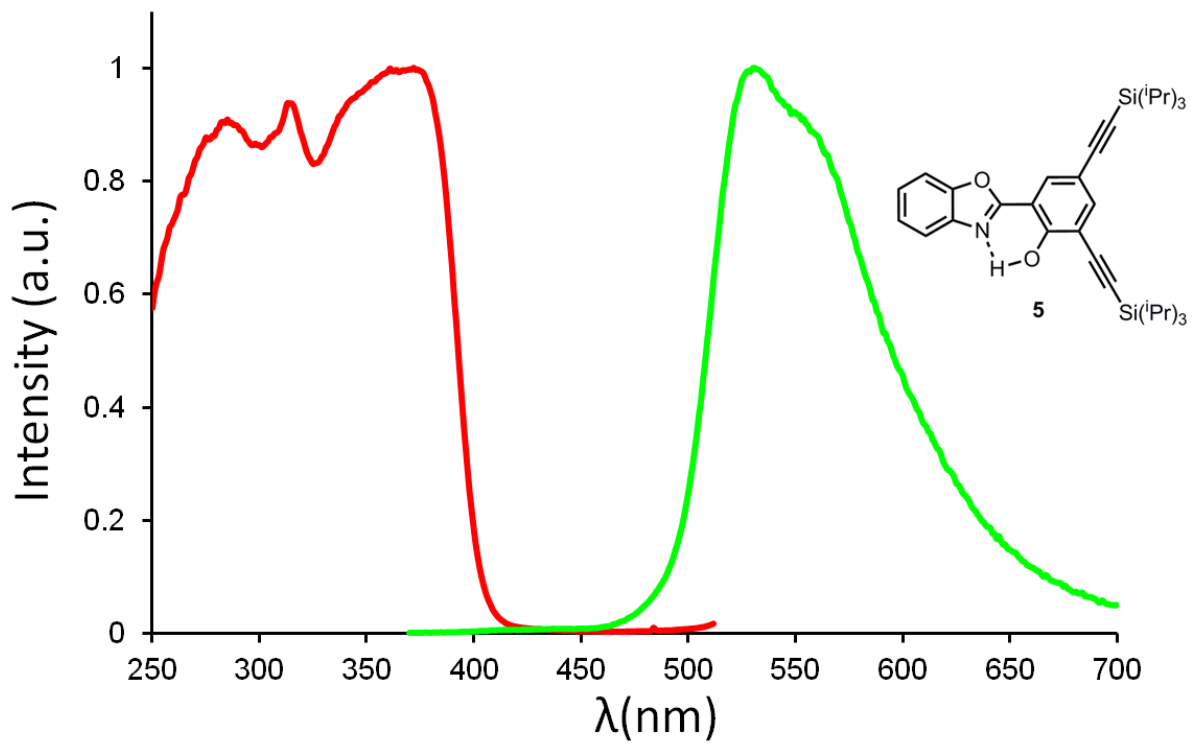




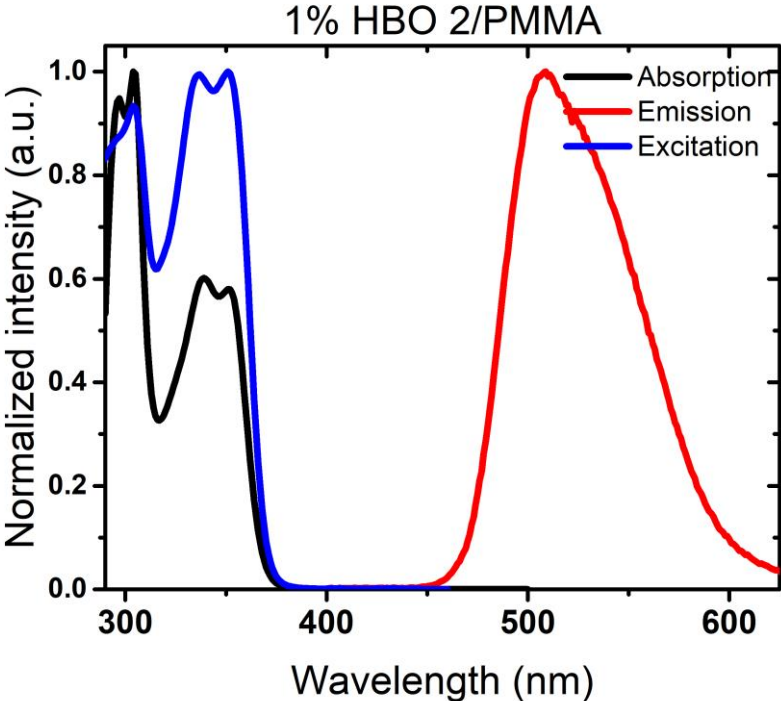
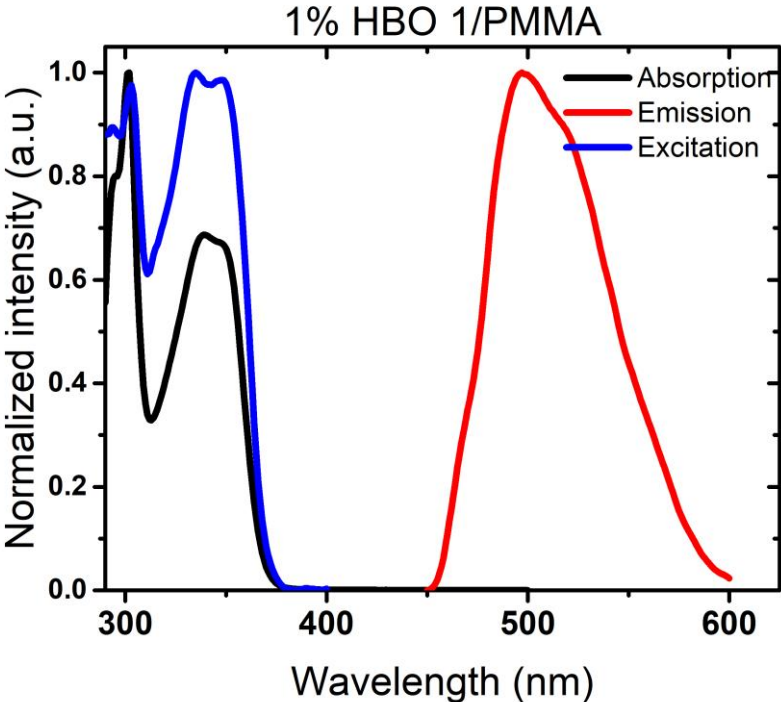
S5.2 Excitation (red) and emission (green) spectra of HBO dyes 1-5 in KBr pellets

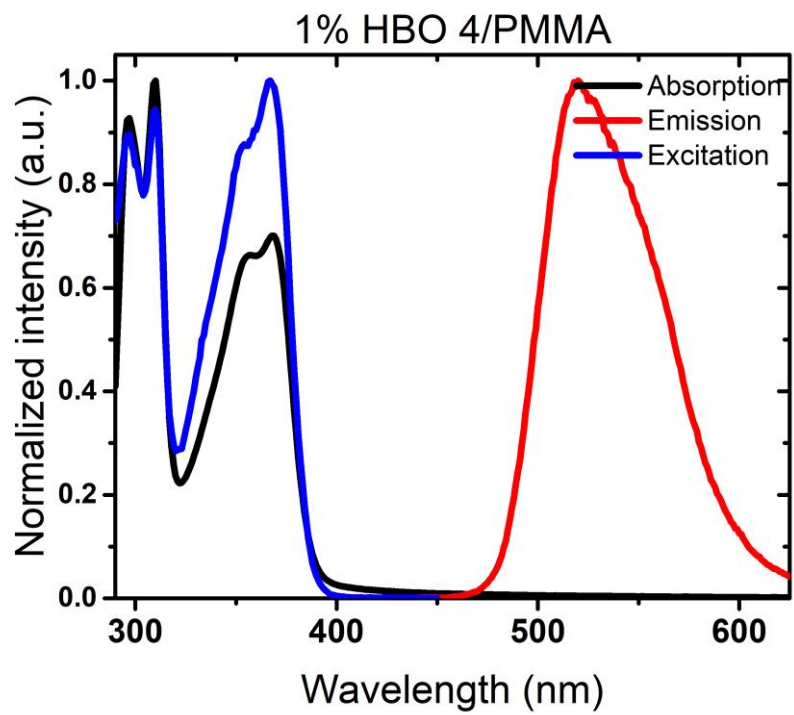
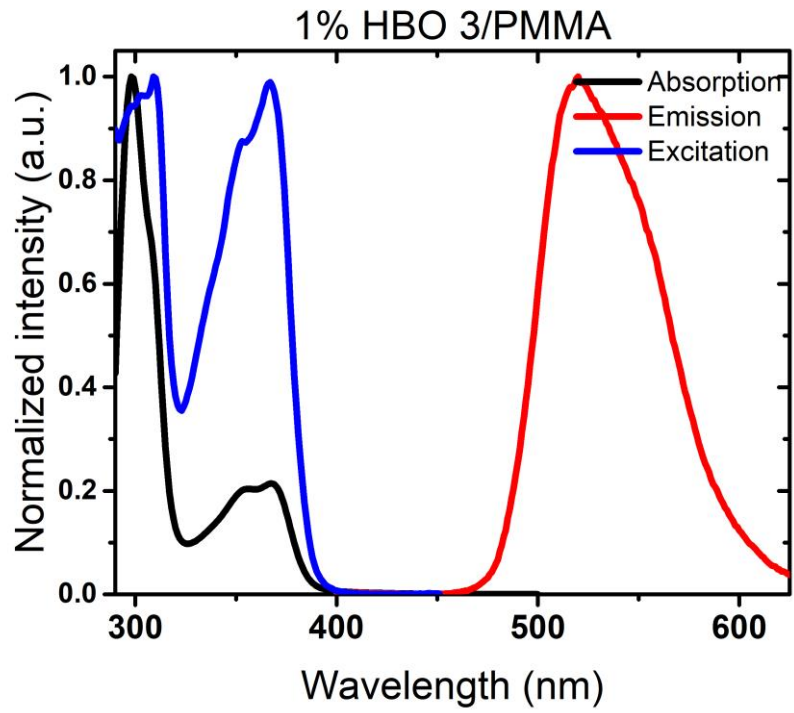


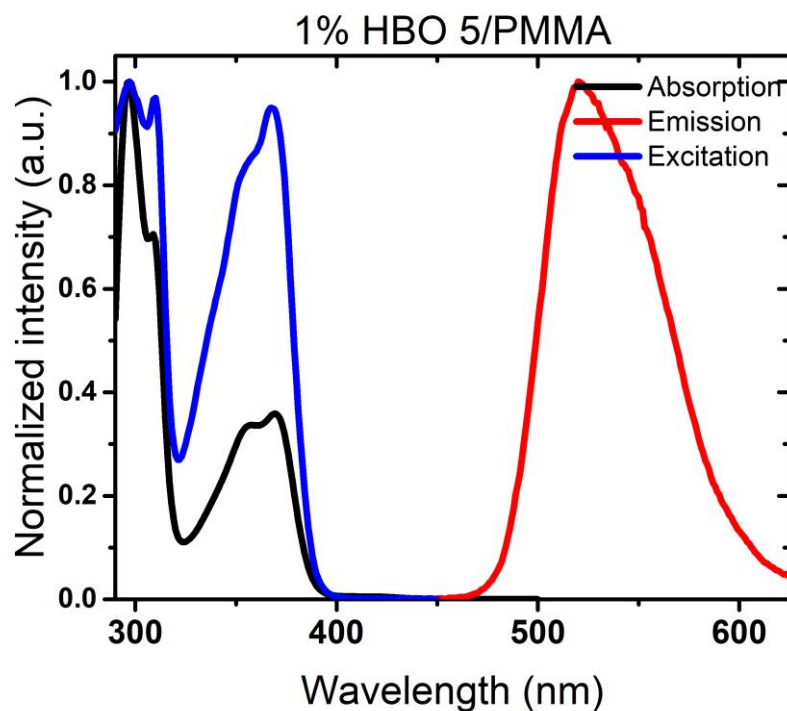




S5.3 Absorption, excitation and emission spectra of HBO dyes 1-5 in PMMA films







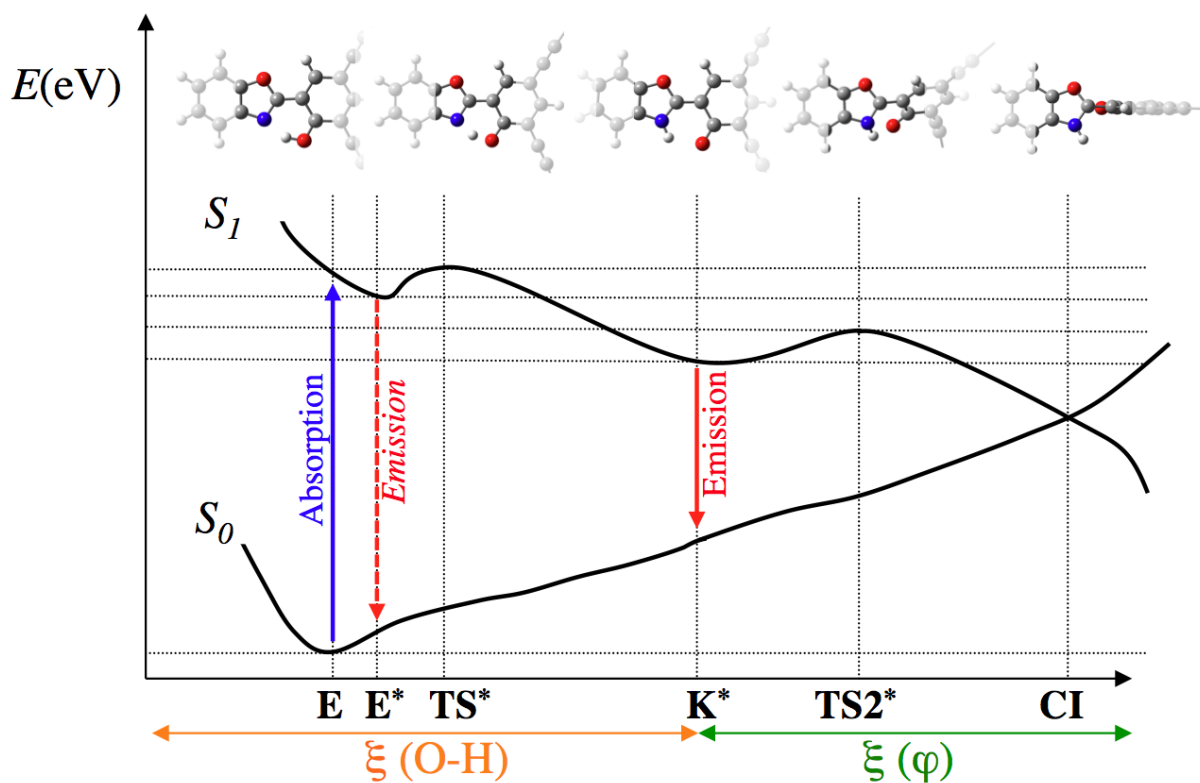
S6 Theoretical calculations

S6.1 Methods

Our computational protocol is based on current state-of-the-art for modeling ES IPT-type reactions as well as the emission and absorption spectra of comparable types of molecules.³ We used a composite approach combining the results of Time-Dependent Density Functional Theory (TD-DFT) and the second-order algebraic diagrammatic construction [ADC(2)] method and investigated the structures as represented on the Scheme on the following page. In this composite approach, detailed in Ref. 3b, the structures and vibrations are determined by using (TD-)DFT geometries obtained with the M06-2X functional, the solvent effects are modeled with the polarizable-continuum model (PCM, here with toluene as solvent)⁴ and the total and transition energies are corrected with ADC(2) to obtain theoretical best estimates. The ADC(2) calculations relied on the Resolution-of-Identity (RI) technique and were performed with default parameters. All DFT/TD-DFT calculations were performed by using Gaussian 16 software,⁵ whereas all ADC(2) calculations were performed by using Turbomole 6.6.⁶ For geometry optimizations, the compact 6-31G(d) atomic basis set has been used,

whereas the extended 6-311+G(2d,p) [*aug-cc-pVTZ*] atomic basis set has been applied for TD-DFT [ADC(2)] transition-energy calculations. The optimized structure of ground and excited states were confirmed by frequency calculations by using analytical Hessian for both the ground and the excited states, which resulted in no imaginary frequency for E, E* and K*, and one imaginary frequency for the transition-state structure corresponding to the proton-transfer (TS*) and K* form twist to the conical intersection (TS2*). To achieve numerical stability in the results, we used a tightened self-consistent field (10^{-10} a.u.) and geometry optimization (10^{-5} a.u.) convergence criteria and the so-called *ultrafine* (99,550) DFT-pruned integration grid during all our TD-DFT calculations. Geometry optimizations and Hessian calculations of the excited states took advantage of the linear-response (LR)⁷ PCM scheme whereas for transition energies the more elaborate corrected LR scheme (cLR)⁸ was used to take into account the change in the cavity polarization upon electron excitation by calculation of excited-state one-electron density. During gradient and Hessian TD-DFT calculations, we applied the *equilibrium* regime of PCM solvation (slow processes), absorption and fluorescence were treated as fast *nonequilibrium* processes. The density difference plots ($\Delta\rho$) were obtained from the difference in the total density of the excited state and the ground state (LR-PCM-TD-DFT calculation), with the former calculated by using so-called Z-vector approach. A contour threshold of 0.008 au was used for the representation.

S6.2 Representation of a typical energy landscape



Scheme S6.1. Representation of the potential energy surface during the ESIP process, with first a proton transfer (O-H reaction coordinate) and next a twist of the structure leading to a conical intersection (CI), back to the ground-state.

S6.3 Density difference plots

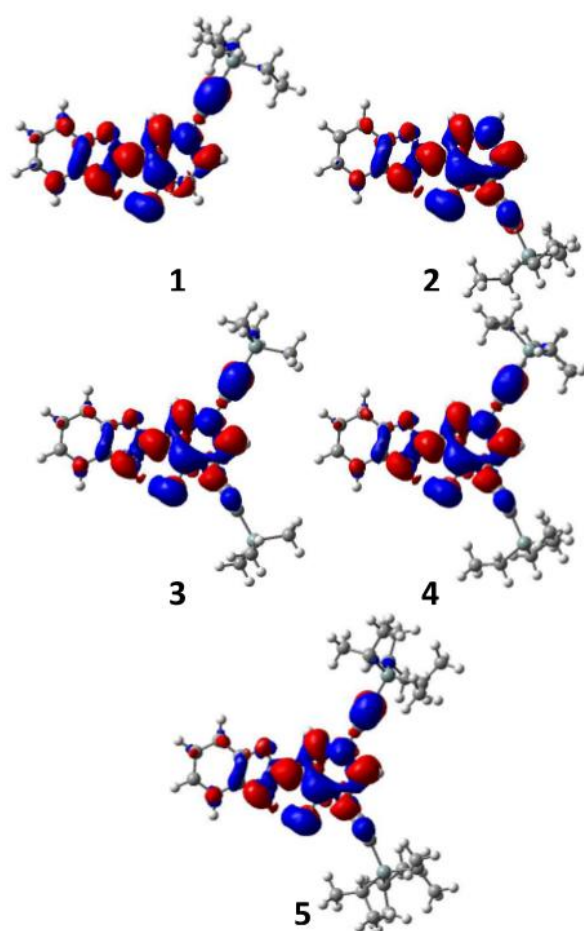


Figure S6.1. Density difference plot corresponding to electronic excitation of HBO 1-5. The blue and red regions respectively correspond to decrease and increase of electronic density upon absorption.

S7 RL Studies

SAMPLE PREPARATION & METHODS FOR RANDOM LASING STUDIES & PHOTODEGRADATION

A series of polymeric thin films doped with HBO dyes were prepared by drop casting method as described elsewhere.¹⁹ Samples were made according to following procedure: commercially available PMMA in powder form ($M_w = 350$ kDa, Sigma Aldrich®) was added to toluene (POCH S.A.) with concentration of 5% w/w (dry weight proportion). This solution was stirred and left for complete polymer dissolution. A separate solutions of HBO dyes in toluene were made with 1% w/w, then mixed with PMMA solution with concentration varying from 1% to 5% w/w (with respect to PMMA). The final solution was stirred for 24h for stabilization preceding deposition on the glass plate by the drop casting technique. Polymeric ESIPT doped films were left in solvent saturated atmosphere for 48h at room temperature for toluene evaporation. For random lasing experiments, the triplet in frequency Nd:YAG nanosecond laser beam (355 nm, 6 ns) was directed through a half-wave plate, polarizer and series of convex and cylindrical lenses incident onto the sample surface, thus obtaining stripe shaped area of illumination with uniform intensity in dimension of 5 mm x 0.5 mm. Emitted light coming from the sample was collected perpendicularly to the investigated layer surface plane by a high resolution Andor Shamrock SR-163 fiber spectrometer in a function of excitation energy density.

For photodegradation measurements we used following definition: a number of pulses upon which the intensity of emission drops by half ($t_{1/2}$). Setup was the same, as for RL studies described previously, alas intensity of input power was constant (2mJ cm⁻²).

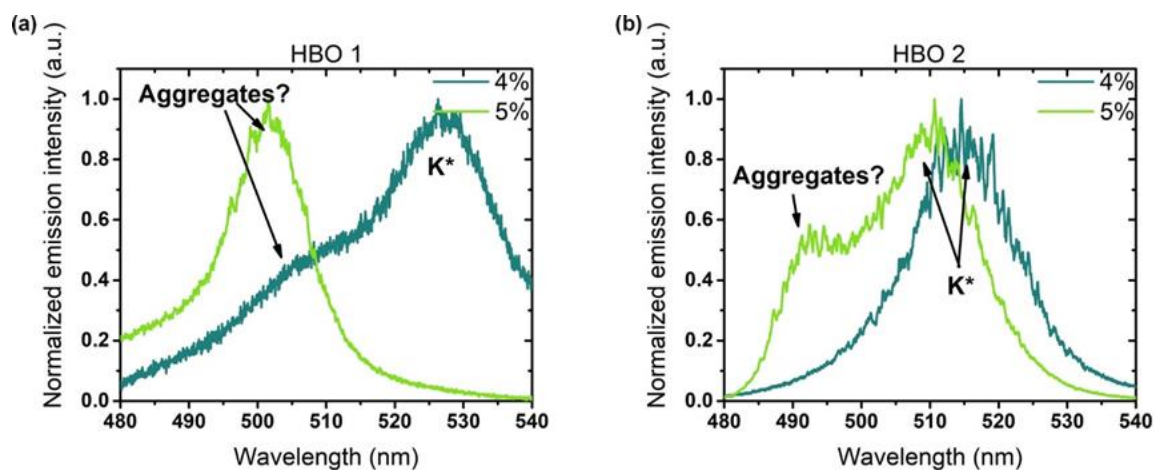


Figure S7.1 Comparison of emission profile of 4% and 5% HBO 1 (a) and HBO 2 (b) in PMMA matrix. For HBO 1 blue-shifted emission from the aggregated form is visible, whereas for HBO 2 dual emission is observed.

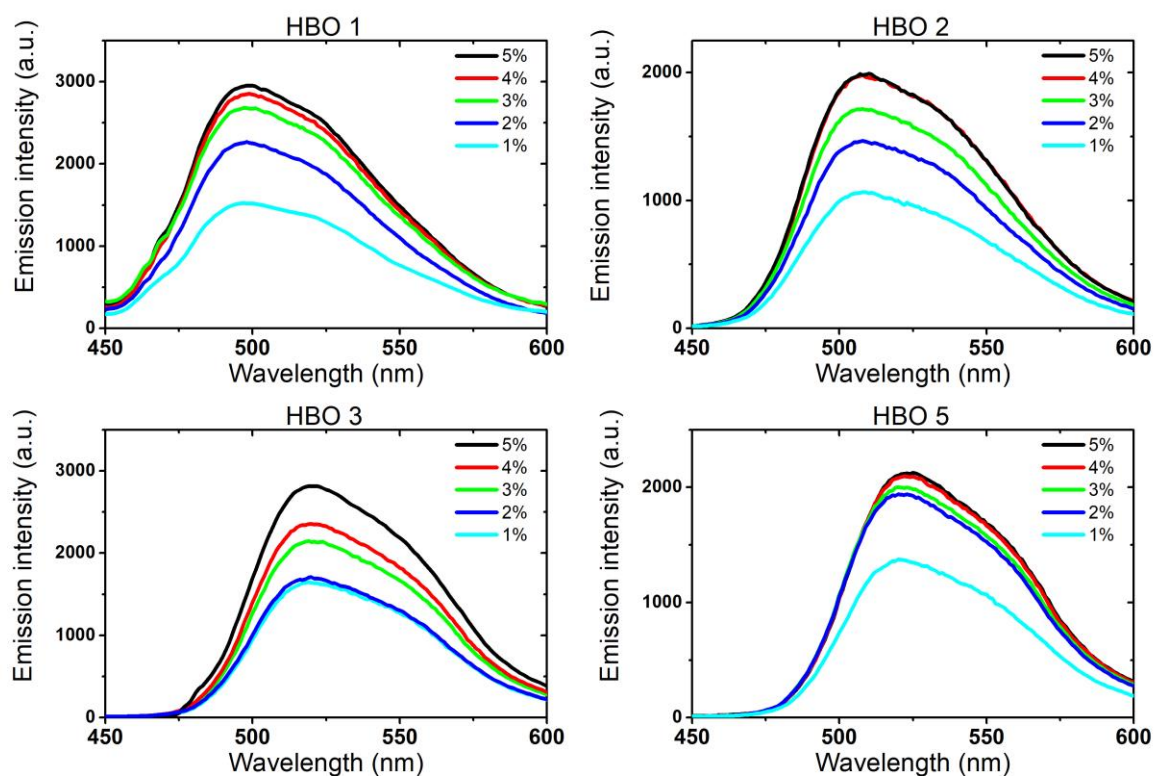


Figure S7.2 Comparison of emission profiles of 1-5% HBO dyes in PMMA matrix.

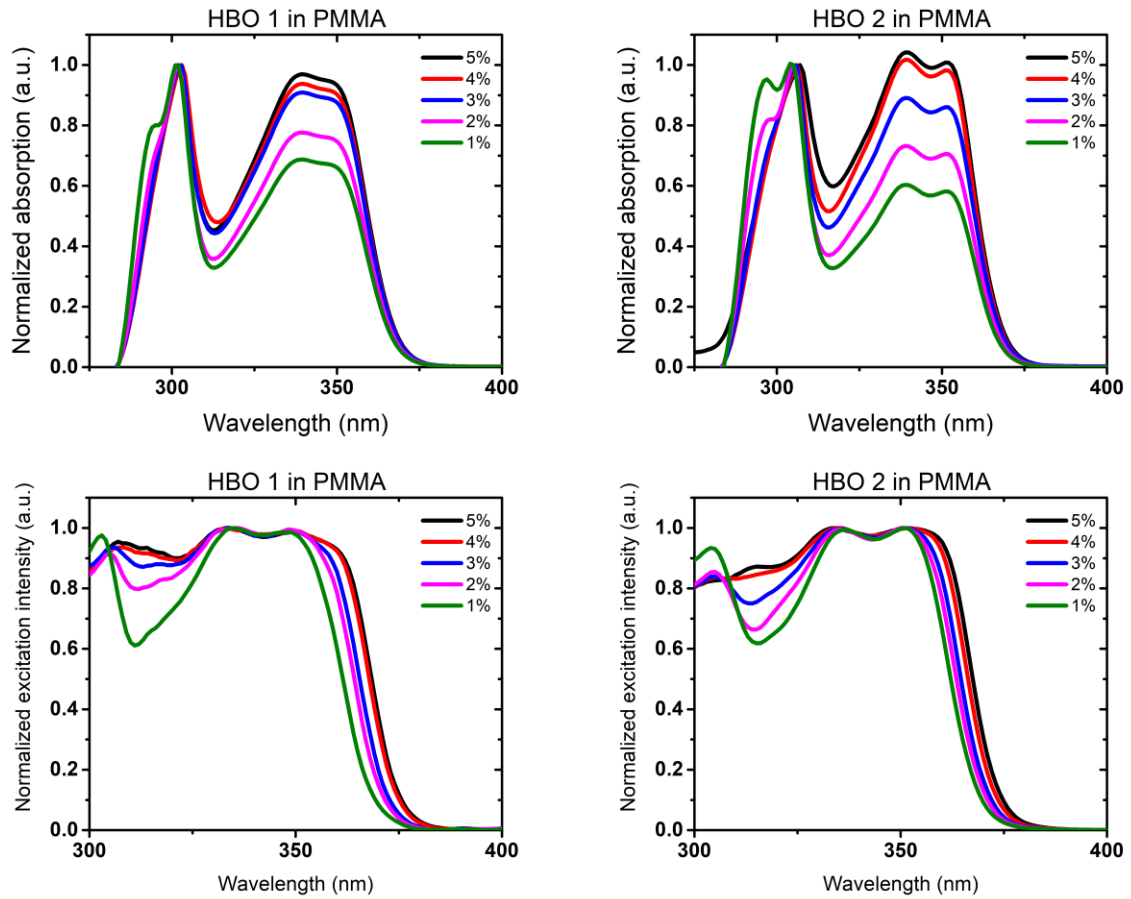


Figure S7.3 Spectroscopic measurements of HBO 1 and 2 doped PMMA films.

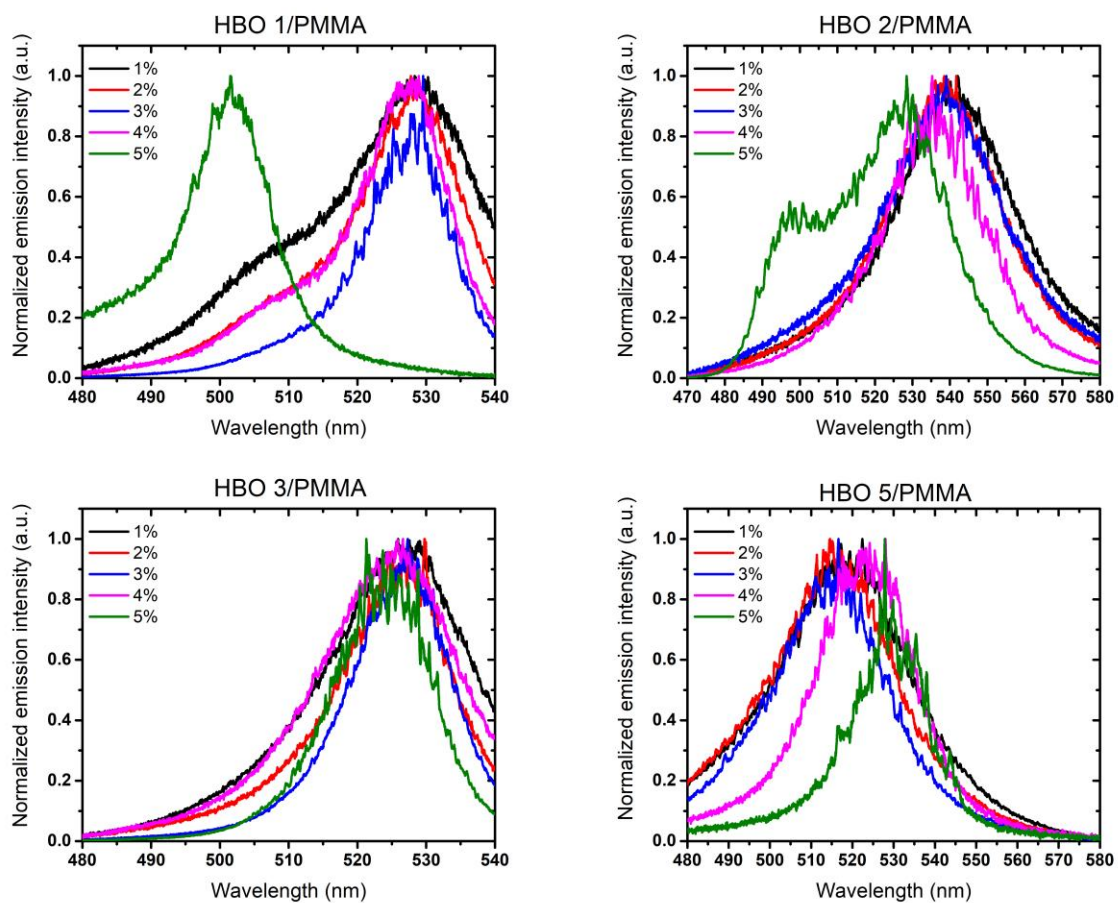


Figure S7.4 Dependence of the light emission spectra on the doping concentration of ESIPT dyes 1-3 and 5 in the PMMA matrix.

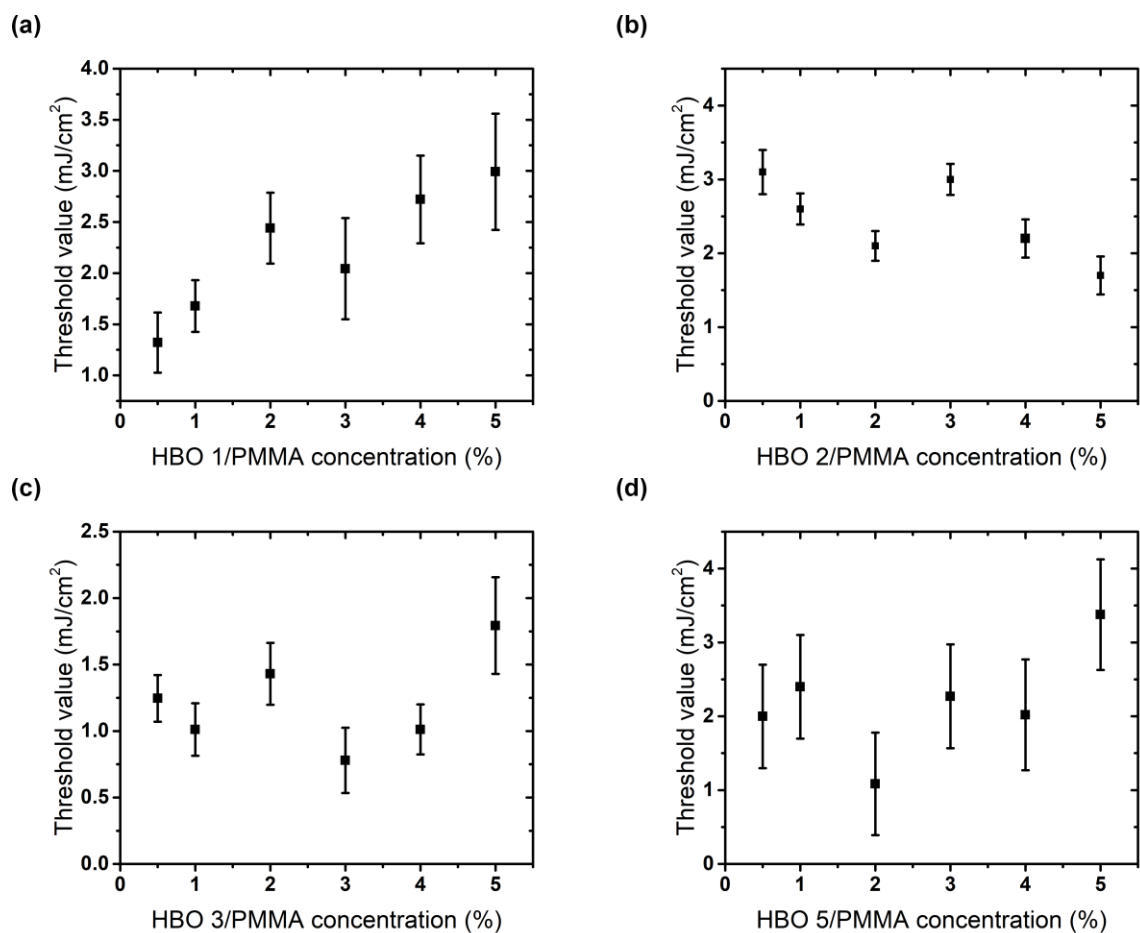


Figure S7.5 Dye concentration influence on RL threshold values for HBO/PMMA thin films. The error bars are noted on the graphs.

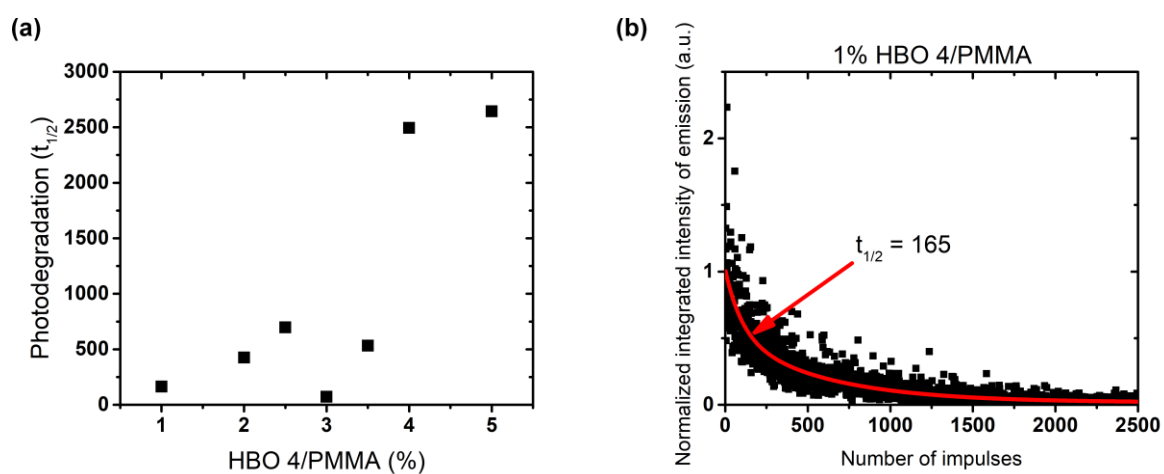


Figure S7.6 (a) Photodegradation results and (b) influence of number of pulses on emission intensity of 1% HBO 4/PMMA thin films.

Table S7.1. Comparison of random lasing properties for dyes **1-5** in PMMA matrix.

We report the maximum emission wavelengths of the keto forms (dyes **1-5**) and of the aggregated forms (dyes **1, 2**), in nm.

Dye	E density at threshold value (mJ/cm ²)	$\lambda_{em,agg}$ (nm)	$\lambda_{em} K^*$ (nm)
1	1.7	500	525
2	2.6	495	540
3	1.0	-	525
4	0.5	-	555
5	1.4	-	525

References

1. J. Massue, G. Ulrich, R. Ziessel, *Eur. J. Org. Chem.*, **2013**, 25, 5701–5709.
2. J. Massue, D. Frath, P. Retailleau, G. Ulrich, R. Ziessel, *Chem. Eur. J.*, **2013**, 19, 5375–5386.
3. (a) M. Raoui, J. Massue, C. Azarias, D. Jacquemin, G. Ulrich, *Chem. Commun.* **2016**, 52, 9216–9219; (b) C. Azarias, S. Budzak, A. D. Laurent, G. Ulrich, D. Jacquemin, *Chem. Sci.* **2016**, 7, 3763–3774; (c) Y. Houari, S. Chibani, D. Jacquemin, A. D. Laurent, *J. Phys. Chem. B* **2015**, 119, 2180–2192; (d) M. Savarese, P. A. Netti, C. Adamo, N. Rega, I. Ciofini, *J. Phys. Chem. B* **2013**, 117, 16165–16173; (e) L. Wilbraham, M. Savarese, N. Rega, C. Adamo, I. Ciofini, *J. Phys. Chem. B* **2015**, 119, 2459–2466.
4. J. Tomasi, B. Mennucci, R. Cammi, *Chem. Rev.* **2005**, 105, 2999–3093

5. Gaussian 16, Revision A.03, M. J. Frisch, G. W. Trucks, H. B. Schlegel, G. E. Scuseria, M. A. Robb, J. R. Cheeseman, G. Scalmani, V. Barone, G. A. Petersson, H. Nakatsuji, X. Li, M. Caricato, A. V. Marenich, J. Bloino, B. G. Janesko, R. Gomperts, B. Mennucci, H. P. Hratchian, J. V. Ortiz, A. F. Izmaylov, J. L. Sonnenberg, D. Williams-Young, F. Ding, F. Lipparini, F. Egidi, J. Goings, B. Peng, A. Petrone, T. Henderson, D. Ranasinghe, V. G. Zakrzewski, J. Gao, N. Rega, G. Zheng, W. Liang, M. Hada, M. Ehara, K. Toyota, R. Fukuda, J. Hasegawa, M. Ishida, T. Nakajima, Y. Honda, O. Kitao, H. Nakai, T. Vreven, K. Throssell, J. A. Montgomery, Jr., J. E. Peralta, F. Ogliaro, M. J. Bearpark, J. J. Heyd, E. N. Brothers, K. N. Kudin, V. N. Staroverov, T. A. Keith, R. Kobayashi, J. Normand, K. Raghavachari, A. P. Rendell, J. C. Burant, S. S. Iyengar, J. Tomasi, M. Cossi, J. M. Millam, M. Klene, C. Adamo, R. Cammi, J. W. Ochterski, R. L. Martin, K. Morokuma, O. Farkas, J. B. Foresman, and D. J. Fox, Gaussian, Inc., Wallingford CT, 2016.
6. TURBOMOLE V6.6 2014, a development of University of Karlsruhe and Forschungszentrum Karlsruhe GmbH, 1989 – 2007, TURBOMOLE GmbH, since 2007; available from <http://www.turbomole.com>
7. R. Cammi, B. Mennucci, *J. Chem. Phys.* **1999**, 110, 9877–9886
8. (a) R. Cammi, S. Corni, B. Mennucci, J. Tomasi, *J. Chem. Phys.* **2005**, 122, 104513;
(b) M. Caricato, B. Mennucci, J. Tomasi, F. Ingrosso, R. Cammi, S. Corni, G. Scalmani, *J. Chem. Phys.* **2006**, 124, 124520.